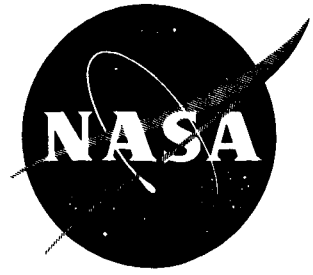

TECHNICAL NOTE

D-25

LARGE-SCALE WIND-TUNNEL TESTS OF AN AIRPLANE MODEL WITH AN UNSWEPT, ASPECT-RATIO-10 WING, FOUR PROPELLERS, AND BLOWING FLAPS

By James A. Weiberg and V. Robert Page

Ames Research Center
Moffett Field, Calif.

NATIONAL AERONAUTICS AND SPACE ADMINISTRATION

WASHINGTON September 1959

NATIONAL AERONAUTICS AND SPACE ADMINISTRATION

TECHNICAL NOTE D-25

LARGE-SCALE WIND-TUNNEL TESTS OF AN AIRPLANE MODEL WITH AN UNSWEPT, ASPECT-RATIO-10 WING, FOUR PROPELLERS, AND BLOWING FLAPS

By James A. Weiberg and V. Robert Page

SUMMARY

An investigation was made of a large-scale model of an airplane having a high-aspect-ratio straight wing, four propellers, and blowing boundary-layer-control flaps and ailerons. Comparison with the results obtained on the same model with two propellers showed that the lift increment due to thrust was proportional to the slipstream velocity and, for a given thrust coefficient, was proportional to the wing area in the slipstream. The drag for a given thrust coefficient and the momentum coefficient required for flow attachment were relatively unaffected by the number of propellers. The downwash variation with angle of attack increased with thrust coefficient approximately in proportion to the increase in lift-curve slope.

INTRODUCTION

Reference 1 has shown that the lift increase resulting from the slipstream of a propeller is dependent on the area and aspect ratio of the wing immersed in the slipstream. For a wing chord small in relation to the slipstream diameter, the lift increase is proportional to the dynamic pressure in the slipstream. As the wing chord is increased in relation to the slipstream diameter, the lift due to the slipstream is reduced to a limiting condition which is proportional to the slipstream velocity. To investigate the effect of slipstream span on the lift increment due to thrust on a wing with high lift flaps, tests were made of the model of reference 2 modified to incorporate four propellers. For the two models, the same total propeller disk area was maintained in the tests made in the Ames 40- by 80-foot wind tunnel. The present results are compared with those of reference 2.

NOTATION

b wing span, ft

c wing chord parallel to plane of symmetry, ft

$\bar{c}$ mean aerodynamic chord, $\frac{2}{S}\int_0^{b/2} c^2 dy$, ft

C_D' drag coefficient,[1] $C_D + T_C'$

C_D drag coefficient including thrust, $\frac{\text{measured drag}}{q_\infty S}$

C_L lift coefficient, $\frac{\text{lift}}{q_\infty S}$

$\bar{C}_L$ C_L for plain wing (no flaps or propellers) at $\alpha = 0^\circ$

ΔC_{L_a} computed lift increment due to aileron deflection (ref. 3)

ΔC_{L_f} computed lift increment due to flap deflection (ref. 3)

ΔC_{L_s} computed lift increment due to slipstream (ref. 1)

C_{l_o} average computed section lift coefficient at the section cut by the slipstream in the absence of the slipstream

C_m pitching-moment coefficient,[2] $\frac{\text{pitching moment}}{q_\infty S \bar{c}}$

C_n local normal-force coefficient determined from integrated pressure distributions

C_μ jet momentum coefficient, $\frac{w_j}{g q_\infty S} V_j$

D propeller diameter, ft

D_s slipstream diameter at 0.25 chord of wing

g acceleration of gravity, 32.2 ft/sec^2

h_j nozzle height, in.

---

[1] With the usual notation, positive thrust is in a negative drag direction.

[2] Pitching moments are presented about a moment center located on the thrust axis below the $0.25\bar{c}$ as shown in figure 1.

i_t angle of stabilizer setting (relative to fuselage reference line), deg

J propeller advance ratio, $\frac{V_\infty}{nD}$

n propeller angular velocity, rps

N number of propellers

p static pressure, lb/sq ft

p' total pressure in flap duct, lb/sq ft

q dynamic pressure, lb/sq ft

R gas constant for air, 1715 $ft^2/sec^2\ {}^oR$

s slipstream velocity factor from elementary momentum theory of propellers so that $V_\infty(1 + s)$ equals the velocity at the 0.25 chord of the wing in the slipstream

S wing area, sq ft

T_d duct temperature, ^oR

T_C' thrust coefficient, $\frac{\text{thrust}}{q_\infty S}$

V velocity, ft/sec

V_j jet velocity assuming isentropic expansion, $\sqrt{\frac{2\gamma}{\gamma-1} RT_d\left[1 - \left(\frac{p_\infty}{p_d'}\right)^{\frac{\gamma-1}{\gamma}}\right]}$, ft/sec

w_j weight rate of air flow through nozzle, lb/sec

y spanwise distance, perpendicular to plane of symmetry, ft

α angle of attack of fuselage center line, deg

δ movable surface deflection measured in plane normal to hinge line, deg

γ ratio of specific heats, 1.4 for air

ϵ downwash angle, deg

Subscripts

a	aileron
f	flap
max	maximum
s	slipstream
u	uncorrected for tunnel-wall effects or strut interference
∞	free-stream conditions

MODEL

The model tested was that used for the tests reported in reference 2 modified to incorporate four propellers. The geometry of the model is shown in figure 1, and a photograph of the model mounted in the wind tunnel is shown in figure 2. Pertinent dimensions of the model are listed in table I.

The blowing boundary-layer-control system on the flaps and ailerons is described in reference 2. The height of the jet nozzle on the flaps and ailerons was 0.060 and 0.040 inches, respectively.

The model was equipped with 4 three-bladed, 4.77-foot-diameter propellers. This propeller diameter was chosen to give the same total propeller disk area as the two-propeller model of reference 2. The geometric characteristics of the blades are shown in figure 3. The blade angle at 0.75 blade radius was set at 21.5°. The propellers were rotated in a clockwise direction viewed from the rear.

TESTS AND CORRECTIONS

The tests were made at free-stream velocities from 51 to 93 feet per second (q_∞ of 3 to 10) corresponding to Reynolds numbers of 1.4 to 2.6 million based on the mean aerodynamic chord of the model of 4.73 feet. The method of determining propeller thrust is described in reference 2. The propeller thrust characteristics are given in figure 4. The data presented in the figures include the direct propeller forces as well as the aerodynamic forces except that the thrust coefficient T_C' has been removed from the measured drag forces (T_C' cos α was assumed equal to T_C').

Corrections for the influence of the tunnel wall were applied to the data as follows:

$$\alpha = \alpha_u + 0.41\ C_L$$

$$C_D = C_{D_u} + 0.0071\ C_L^2$$

$$C_m = C_{m_u} + 0.020\ C_L \text{ (tail on only)}$$

No corrections were made for strut tares or strut interference.

RESULTS AND DISCUSSION

The lift, drag, and pitching-moment characteristics of the model are presented in figures 5(a) to 5(n). The data in figure 5 are for the model with tail removed and with the tail at an incidence of 4.3° (except fig. 5(i) where $i_t = 9^\circ$). Data for flaps 0° and 60° and a tail incidence of -3° are compared in figure 6 with data from reference 2 for the two-propeller model.

Lift Characteristics

The lift due to thrust at a given angle of attack (fig. 6) was greater for the model with four propellers than with two propellers in proportion to the wing area immersed in the slipstream.

The lift characteristics of the four-propeller model for various flap deflections are presented in figure 7. Shown in this figure is the variation with thrust coefficient of maximum lift coefficient, lift-curve slope, and lift coefficient at 0° angle of attack. The measured lift increase at 0° angle of attack resulting from the propeller slipstream is compared in figure 8 with values computed by the theory of reference 1. The values given are increments, ΔC_L, above the plain wing value for 0° angle of attack.[3] For flaps deflected, a flap lift increment computed

---

[3] $\Delta C_{L_{experimental}} = C_L - \bar{C}_L = C_L - 0.55$

$$\Delta C_{L_{computed}} = \Delta C_{L_f} + \Delta C_{L_a} + \Delta C_{L_s}$$

for ΔC_{L_s} proportional to V_s

$$\Delta C_{L_s} = N \frac{D_s c_s}{S} C_{l_o} s$$

for ΔC_{L_s} proportional to q_s

$$\Delta C_{L_s} = N \frac{D_s c_s}{S} C_{l_o} (2s + s^2)$$

from reference 3 has been added to the computed lift due to slipstream. When attached flow is maintained on the flap, the experimental data agree closely with a computed value proportional to the slipstream velocity. For the propeller diameter to wing chord ratio of the present model, these results appear to agree with the results of reference 1. To obtain higher lift increments approaching values proportional to the slipstream dynamic pressure, the results of reference 1 indicate that the wing span covered by the propeller should be of the order of five to six times the wing chord. This ratio for the present model is approximately 2.

A comparison of the measured lift-curve slope with that computed by the method of reference 1 is shown in figure 9. Approximately half of the increase in lift-curve slope with thrust coefficient results from the lift component of thrust, $T_C' \sin \alpha$. Theory predicts with reasonable accuracy the lift-curve slope increase resulting from the propeller slipstream.

Drag Characteristics

The comparison shown in figure 6 indicates that the drag of the model for a given thrust coefficient and lift coefficient (away from maximum lift) was relatively unaffected by the number of propellers even at the high thrust coefficients where there are large differences in span loading (fig. 10).

Pitching-Moment Characteristics

The downwash at the tail was determined from the tail pitching moment and the measured horizontal-tail effectiveness.[4] A value of $q_{tail}/q_\infty = 1.0$ determined from flow surveys at the tail was used. These surveys included measurements of the downwash which agreed reasonably well with the downwash computed from the pitching-moment data.

The variation of downwash with angle of attack for various flap deflections and thrust coefficients is presented in figure 11. A comparison of the downwash for a flap deflection of 60° with values for the two-propeller model is shown in figure 12. The downwash at a given angle of attack for the four-propeller model is shown in figure 13 to be roughly in proportion to the lift coefficient. The increase in the downwash variation with angle of attack $d\epsilon/d\alpha$ with thrust coefficient

[4]The downwash and tail effectiveness were determined from pitching-moment data at tail incidences other than those presented herein. These data were at tail incidences that resulted in angles of attack below the maximum for stall of the horizontal tail.

is shown in figure 14. The increase in $d\epsilon/d\alpha$ with T_C' is roughly proportional to the increase in lift-curve slope.

Blowing Momentum Flow Requirements

A comparison of the momentum flow requirements for the flaps on the two- and four-propeller models is shown in figure 15. The values of C_{μ_f} required for flow attachment determined from observations of static pressures on the flap are indicated by tick marks on the curves. The C_μ required for flow attachment was relatively unaffected by the amount of flap span immersed in the propeller slipstream. This result would be expected based on the data of reference 2 which showed that the flap momentum flow requirements were unaffected by thrust coefficient.

CONCLUSIONS

A comparison of the results of tests of a model with two propellers with one having four propellers showed that the lift increment due to thrust was proportional to the slipstream velocity and, for a given thrust coefficient, was proportional to the wing area in the slipstream. The drag for a given thrust coefficient and the blowing momentum coefficient for flow attachment on the flap were relatively unaffected by the number of propellers. For both the four- and two-propeller models, the downwash variation with angle of attack increased with thrust coefficient approximately in proportion to the increase in lift-curve slope.

Ames Research Center
National Aeronautics and Space Administration
Moffett Field, Calif., Apr. 22, 1959

REFERENCES

1. Smelt, R., and Davis H.: Estimation of Increase in Lift Due to Slipstream. R. & M. No. 1788, British, 1937.

2. Griffin, Roy N., Jr., Holzhauser, Curt A., and Weiberg, James A.: Large-Scale Wind-Tunnel Tests of an Airplane Model With an Unswept, Aspect-Ratio-10 Wing, Two Propellers, and Blowing Flaps. NASA MEMO 12-3-58A. 1958.

3. DeYoung, John: Theoretical Symmetric Span Loading Due to Flap Deflection for Wings of Arbitrary Plan Form at Subsonic Speeds. NACA Rep. 1071, 1952.

TABLE I.- GENERAL GEOMETRIC DIMENSIONS OF THE MODEL

Dimension	Wing	Horizontal surface	Vertical surface
Area, sq ft	205.4	56.5	30.6
Span, ft	45.00	16.03	7.19
$\bar{c}$, ft	4.73	3.50	4.68
Aspect ratio	9.86	4.55	1.69
Taper ratio	.50	.45	.55
Geometric twist, deg	4.8 (washout)	0	0
Dihedral from reference plane, deg	0.8	0	- - -
Incidence from reference plane, deg	8.3	- - -	- - -
Section profile (constant)	NACA 23017	NACA 0012	NACA 0012
Root chord, ft	6.07	4.61	5.88
Tip chord, ft	3.06	2.54	2.65
Sweep of leading edge, deg	2	12	24
Tail length, ft	- - -	[1]18.01	- - -

[1]Distance from 0.25 $\bar{c}$ of wing to 0.25 $\bar{c}$ of horizontal tail.

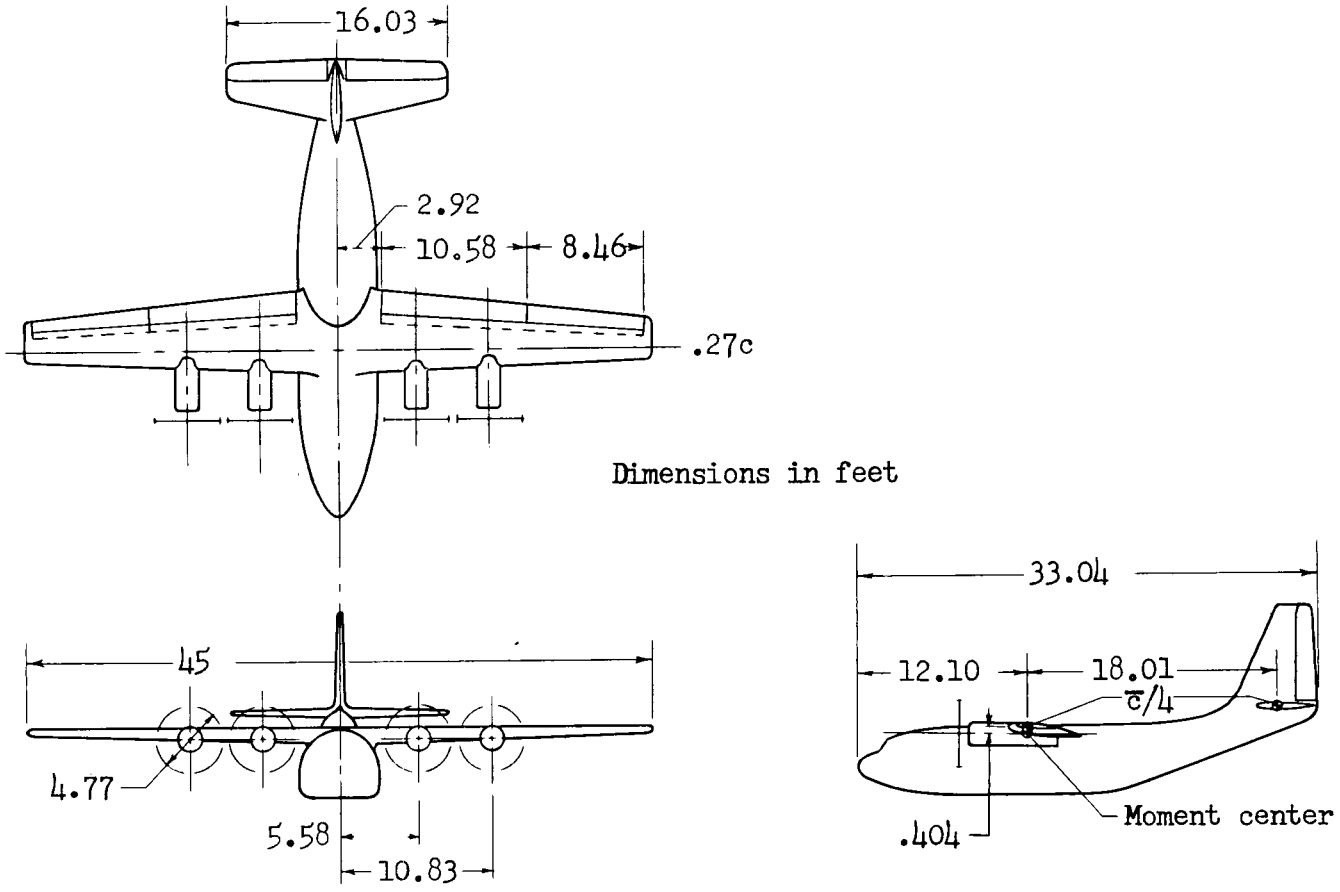

Figure 1.- Geometry of the model.

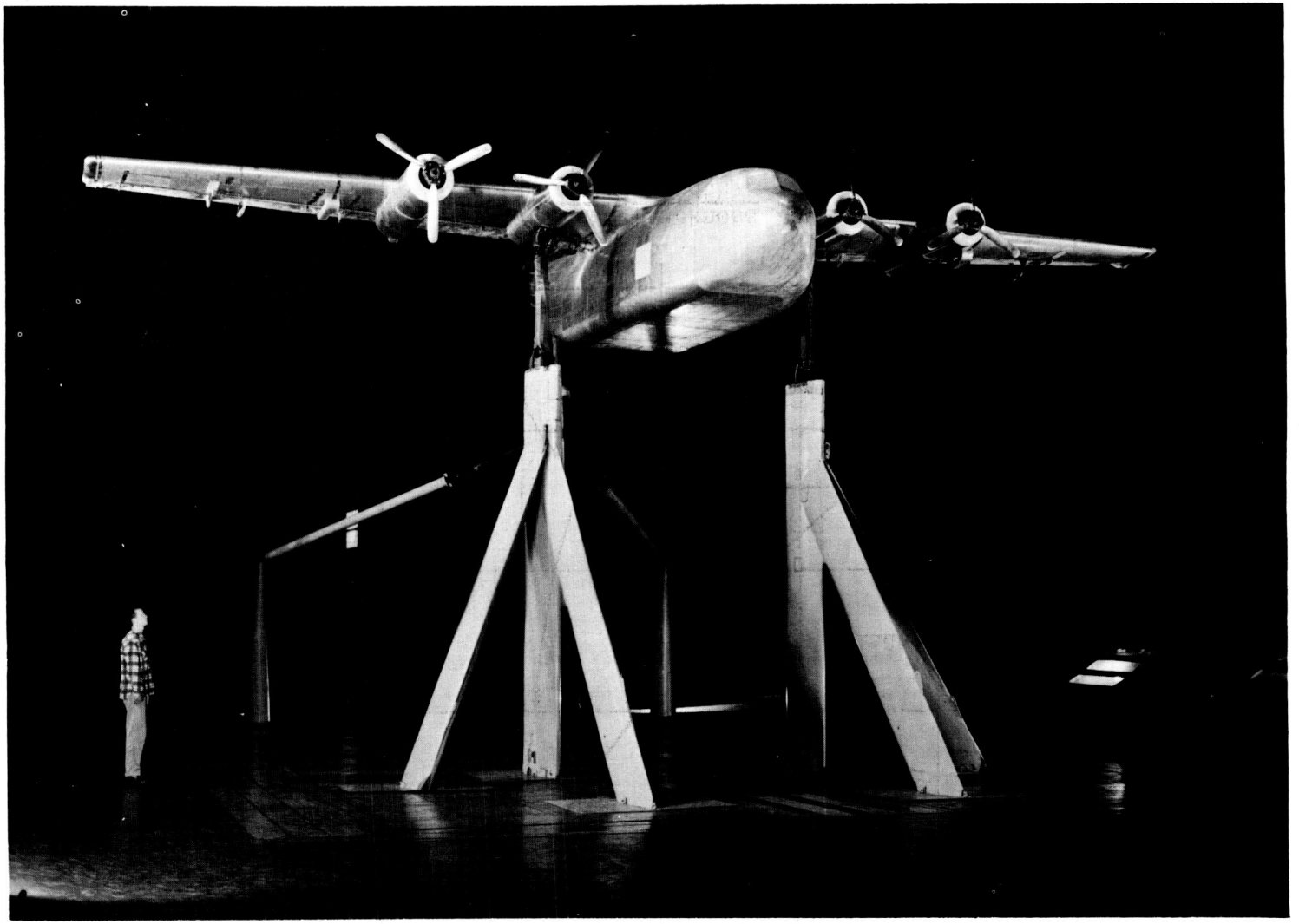

A-23743

Figure 2.- The model mounted in the Ames 40- by 80-foot wind tunnel.

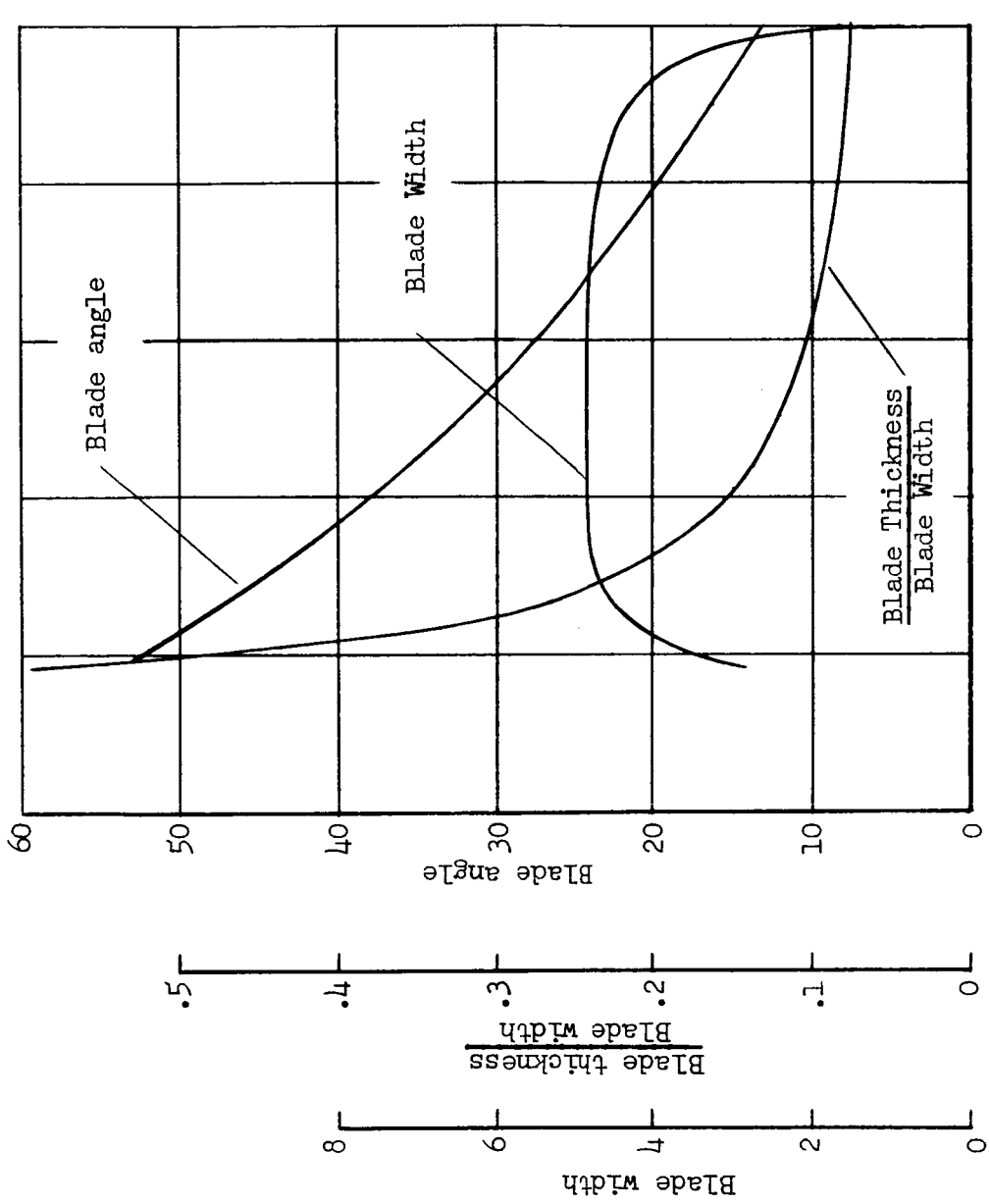

Figure 3.- Propeller-blade form curves.

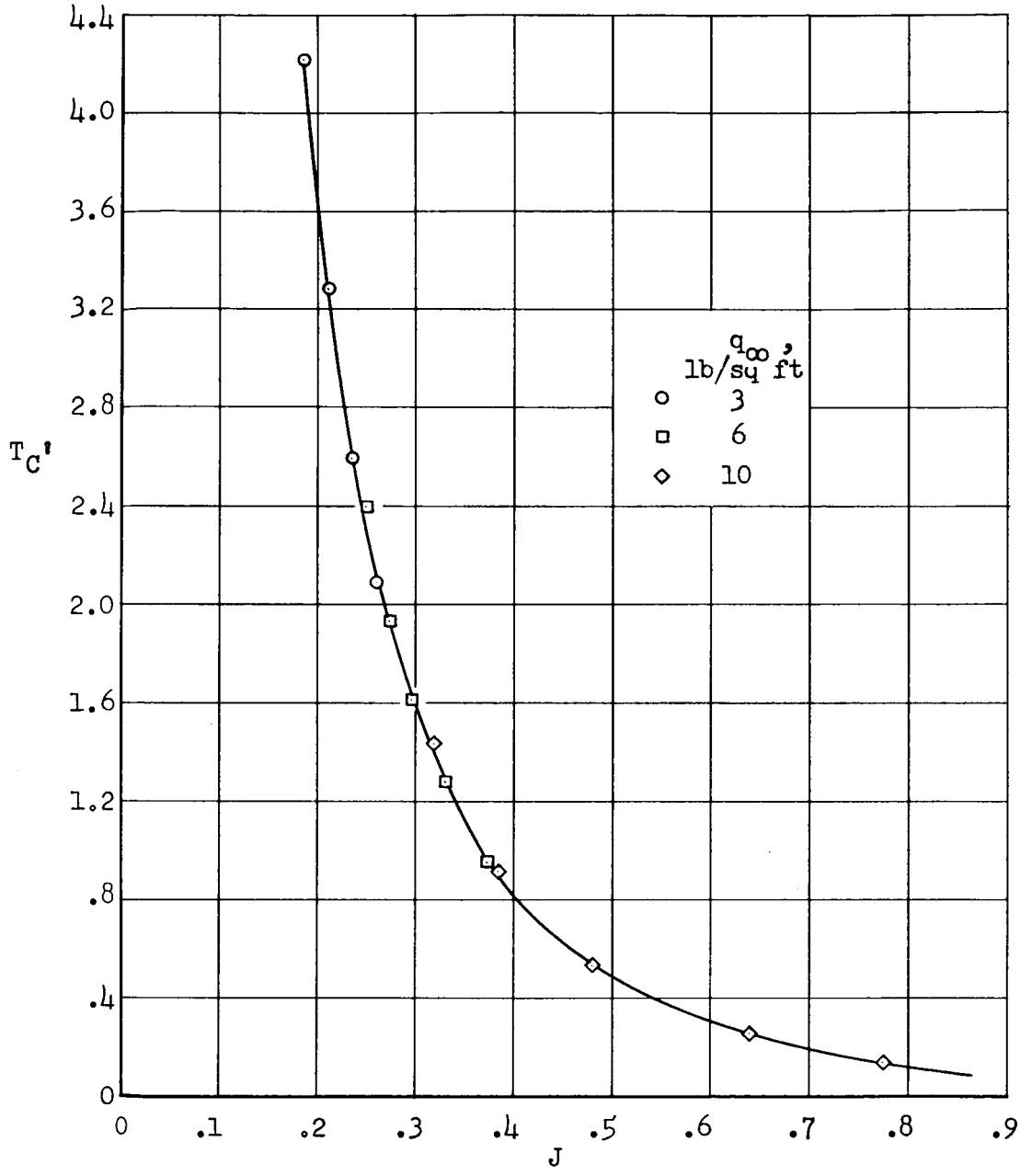

Figure 4.- Thrust characteristics.

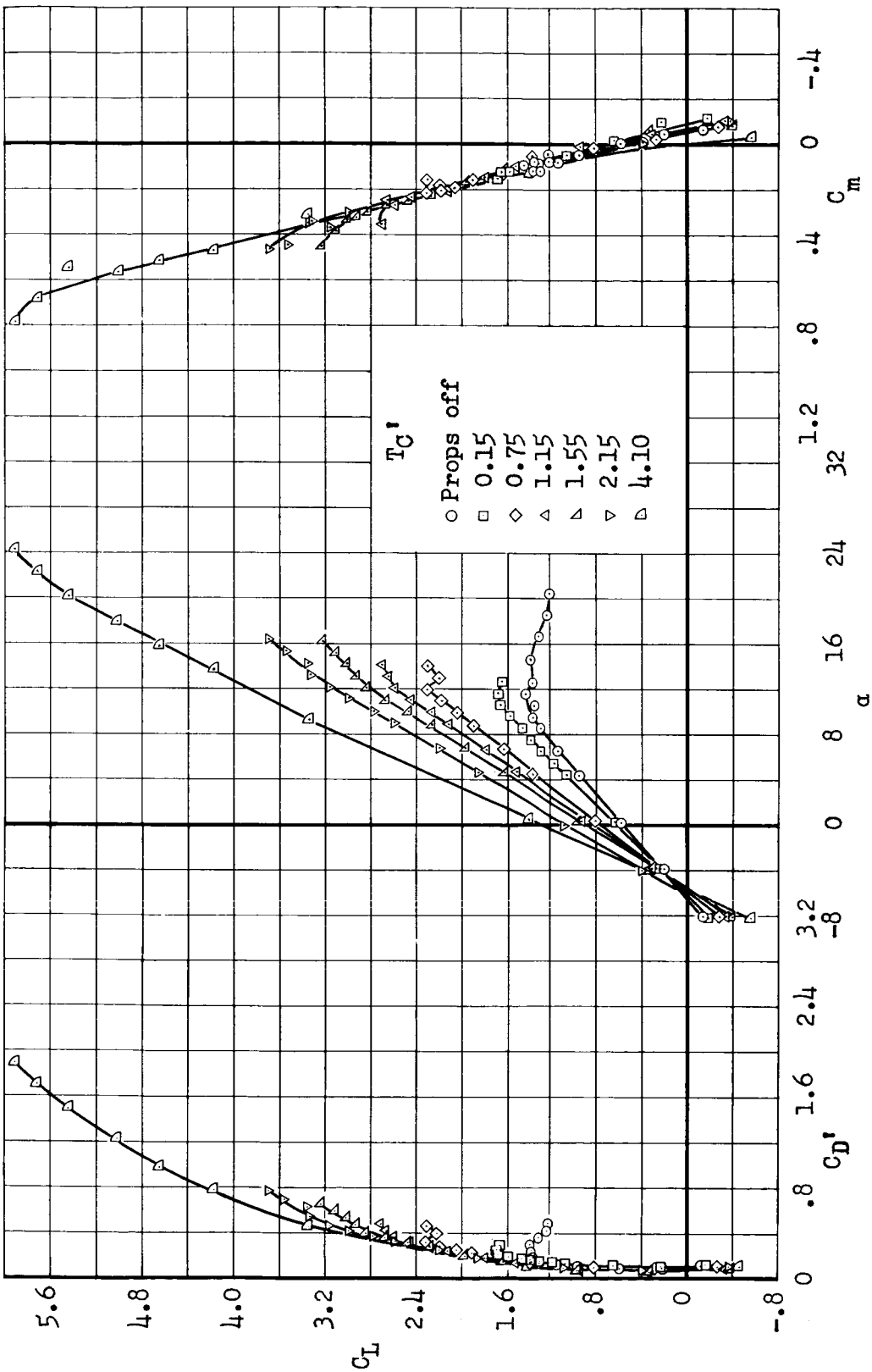

(a) $\delta_f = \delta_a = 0^o$; tail off (horizontal and vertical surfaces).

Figure 5.- Effect of thrust coefficient on the aerodynamic characteristics of the model.

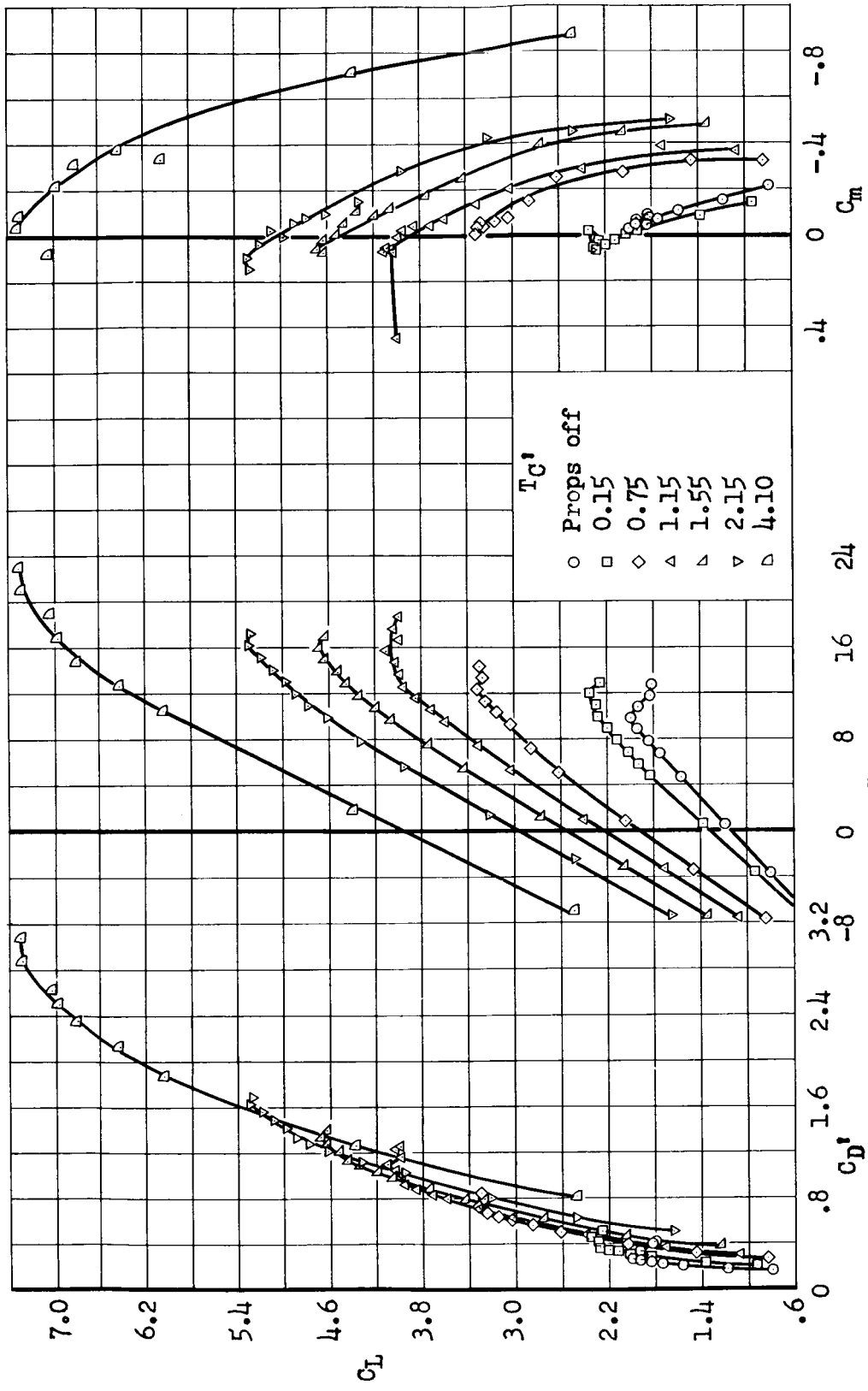

(b) $\delta_f = 40^o$; $\delta_a = 0^o$; $C_{\mu_f} = C_{\mu_a} = 0$; tail off.

Figure 5.- Continued.

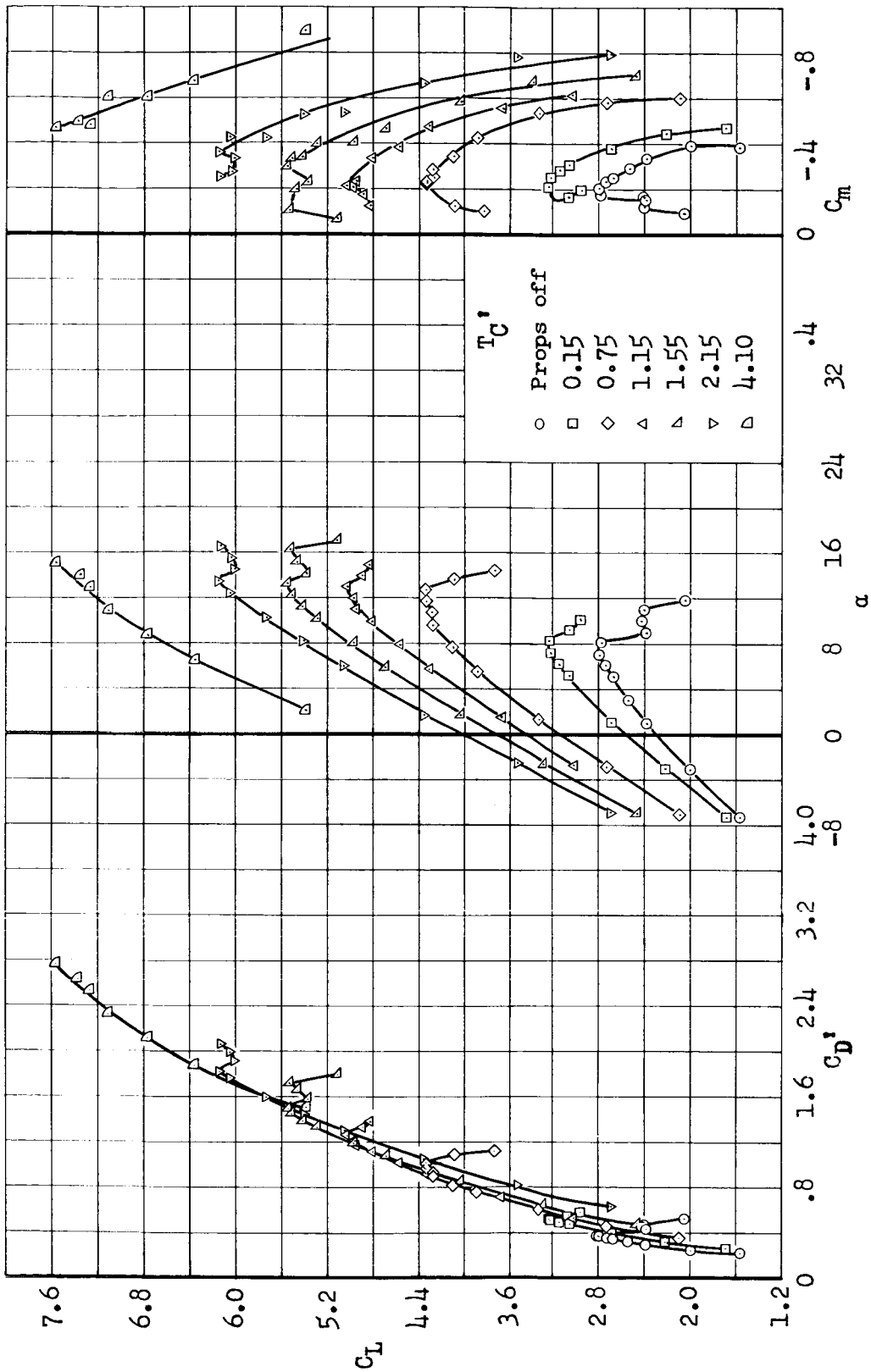

(c) $\delta_f = 40^o$; $\delta_a = 30^o$; $C_{\mu_f} = 0.024$; $C_{\mu_a} = 0.006$; tail off.

Figure 5.- Continued.

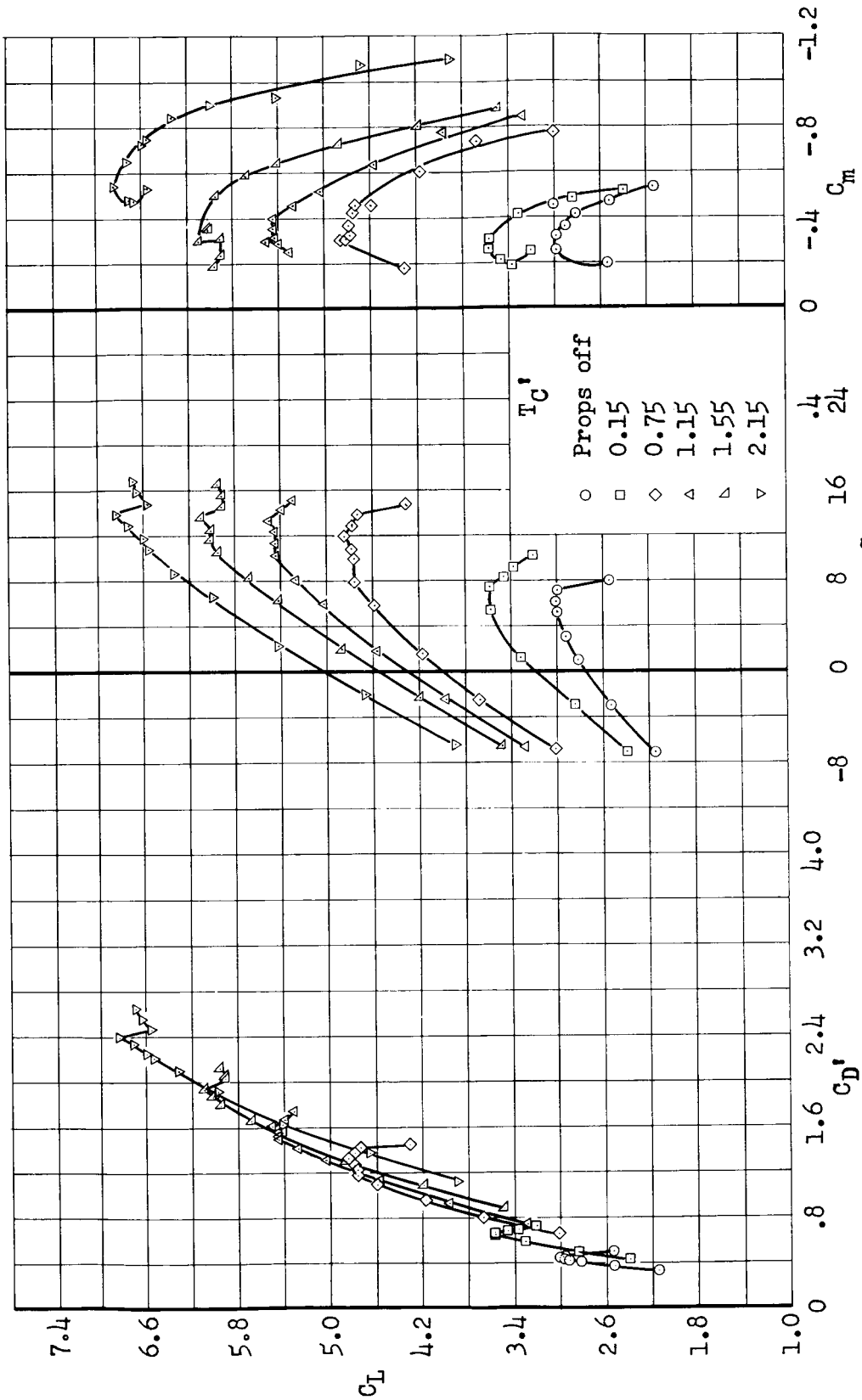

(d) $\delta_f = 60^\circ$; $\delta_a = 30^\circ$; $C_{\mu_f} = 0.029$; $C_{\mu_a} = 0.006$; tail off.

Figure 5.- Continued.

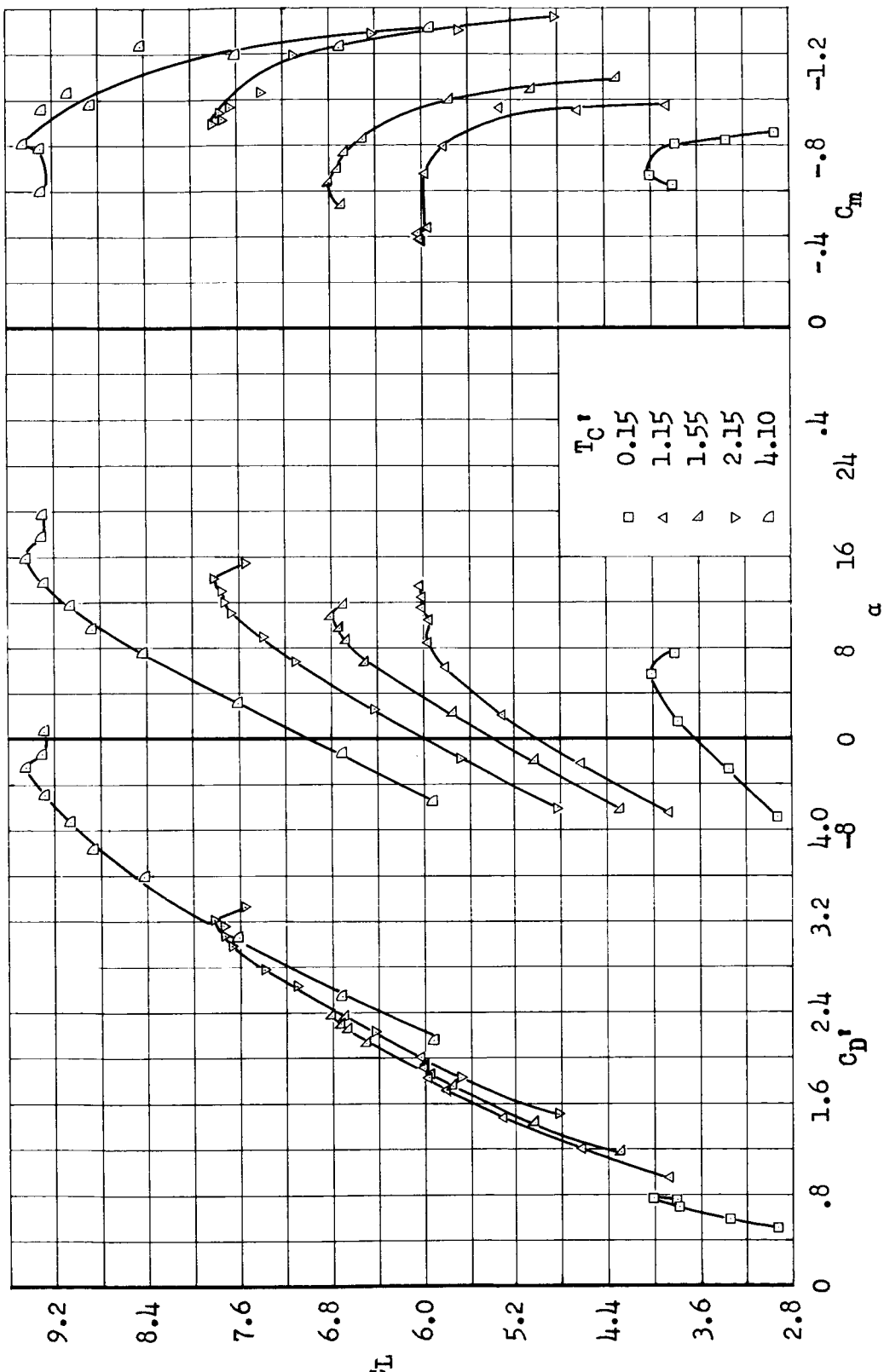

(e) $\delta_f = 60^\circ$; $\delta_a = 30^\circ$; $C_{\mu_f} = 0.080$; $C_{\mu_a} = 0.006$; tail off.

Figure 5.- Continued.

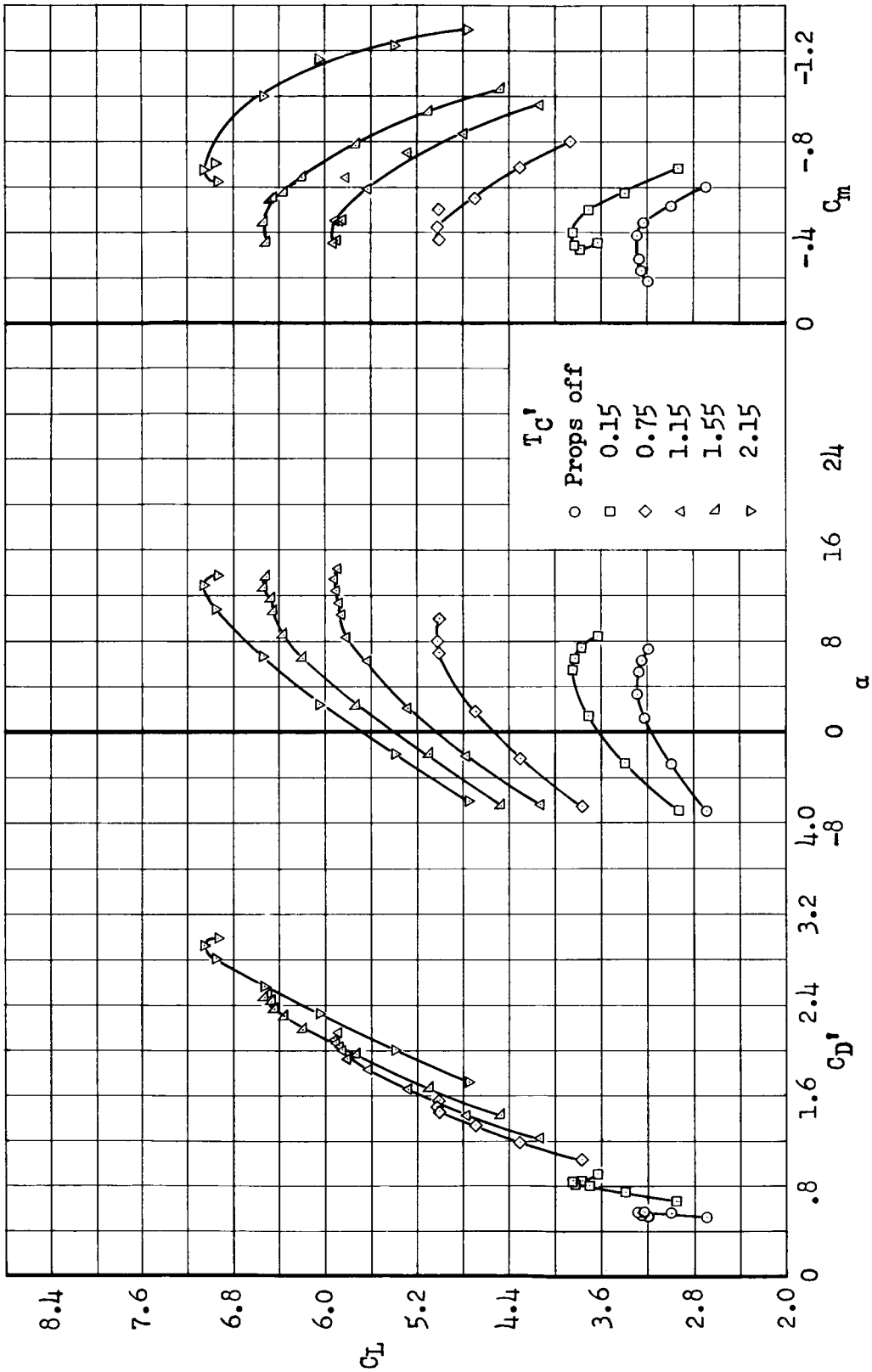

(f) $\delta_f = 80^o$; $\delta_a = 30^o$; $C_{\mu_f} = 0.049$; $C_{\mu_a} = 0.006$; tail off.

Figure 5.- Continued.

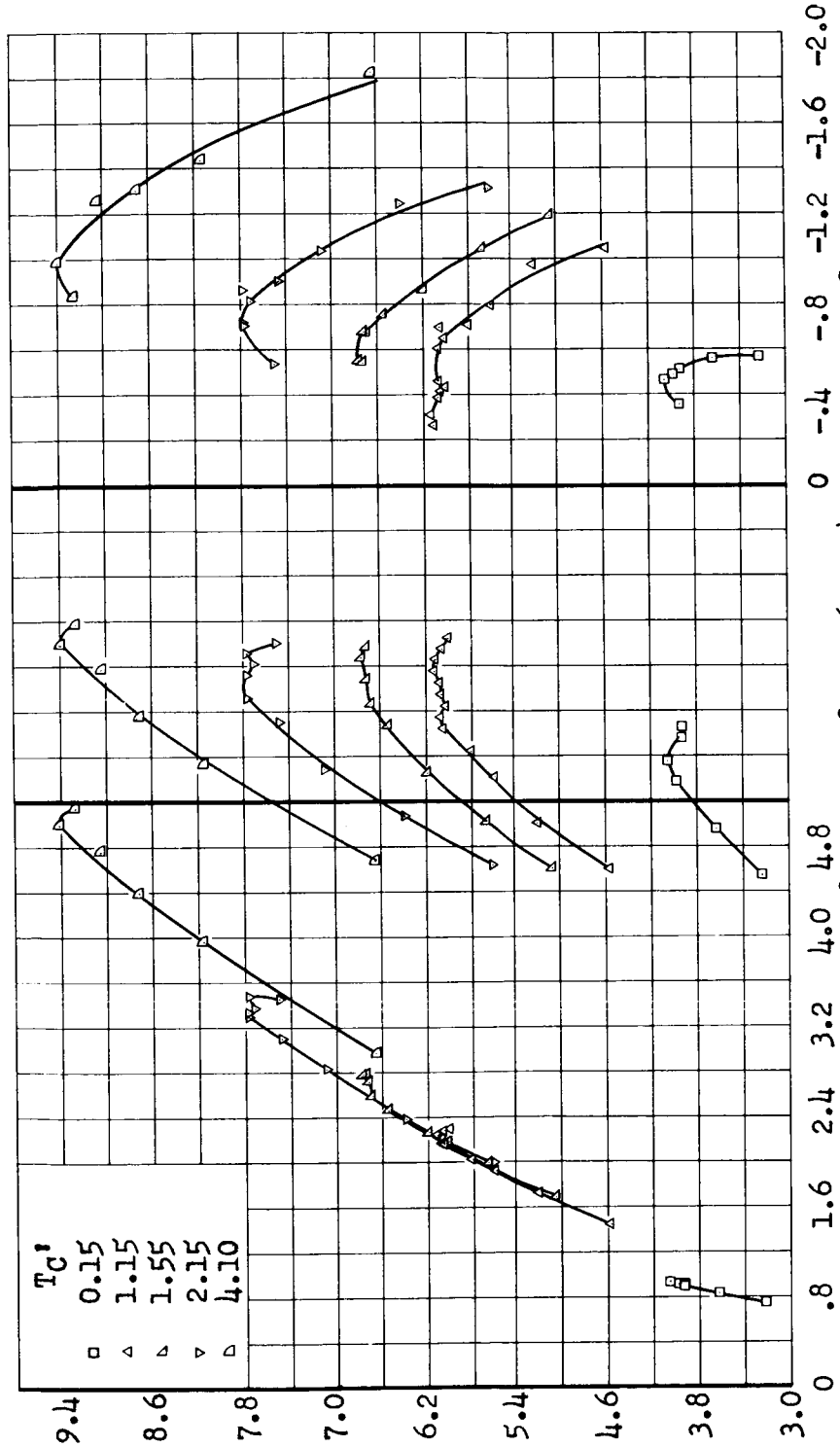

(g) $\delta_f = 80°$; $\delta_a = 30°$; $C_{\mu_f} = 0.08$; $C_{\mu_a} = 0.006$; tail off.

Figure 5.- Continued.

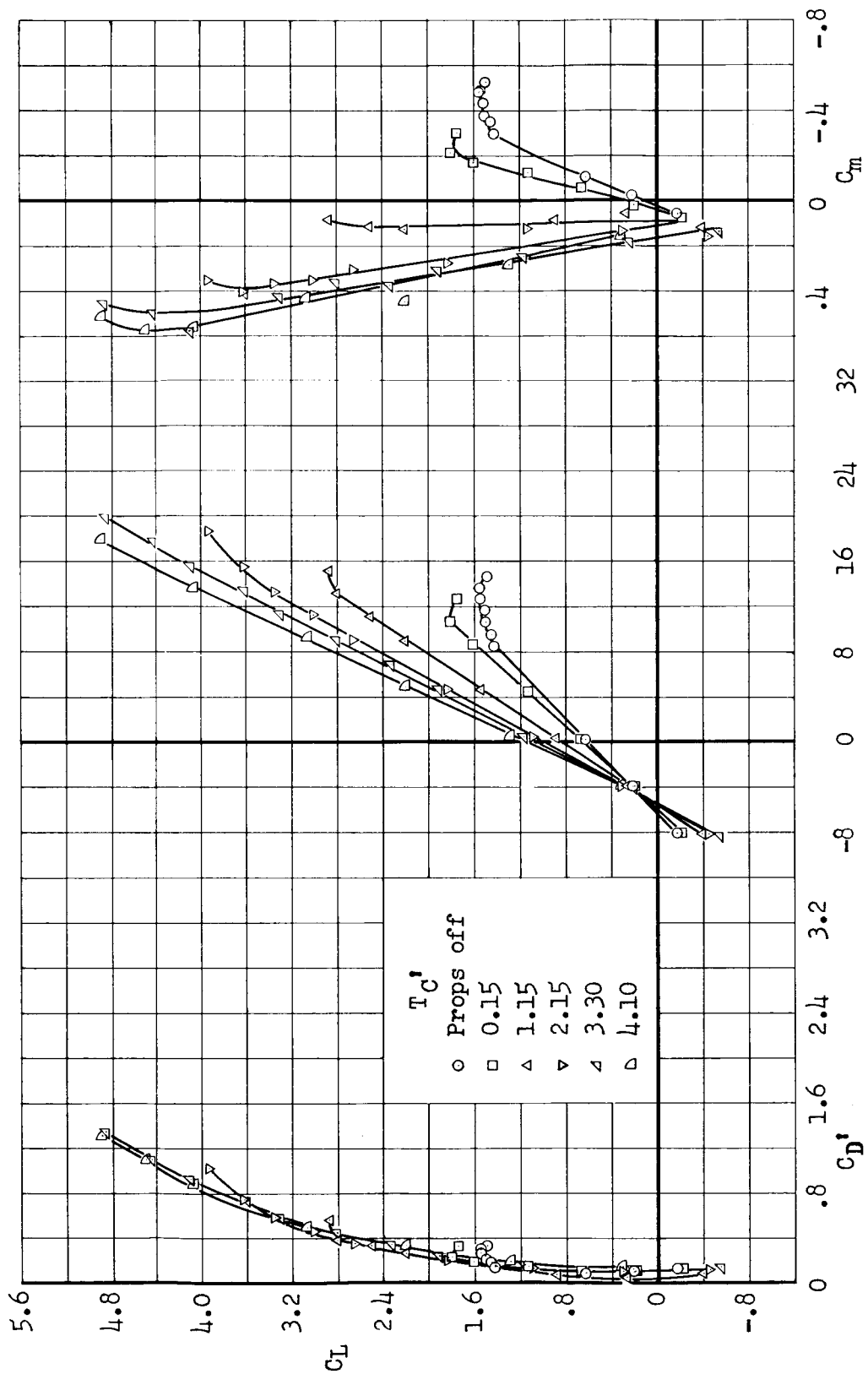

(h) $\delta_f = \delta_a = 0^\circ$; $C_{\mu_f} = C_{\mu_a} = 0$; $i_t = 4.3^\circ$.

Figure 5.- Continued.

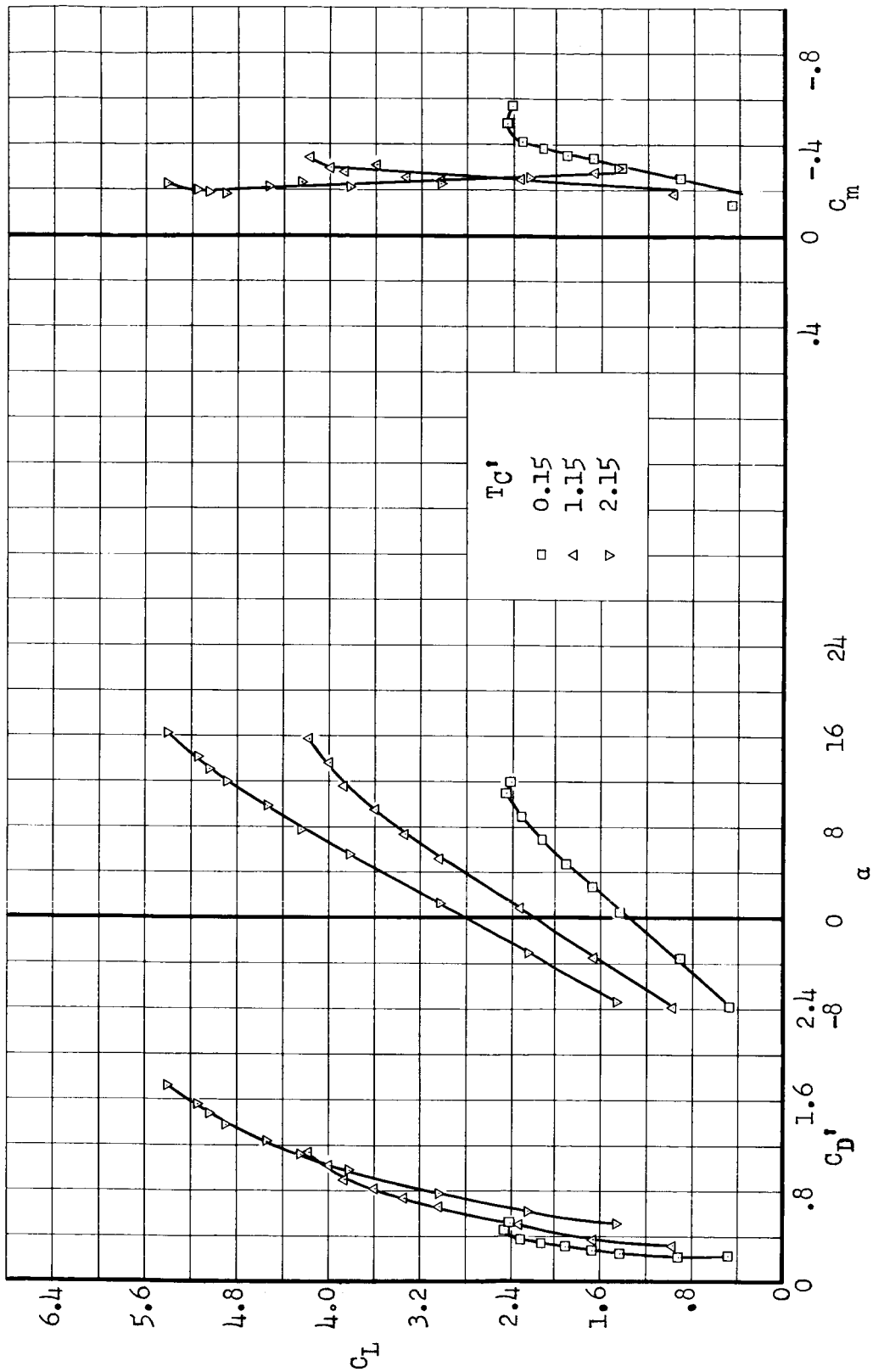

(i) $\delta_f = 40^\circ$; $\delta_a = 0^\circ$; $C_{\mu_f} = C_{\mu_a} = 0$; $i_t = 9^\circ$; vertical-tail off.

Figure 5.- Continued.

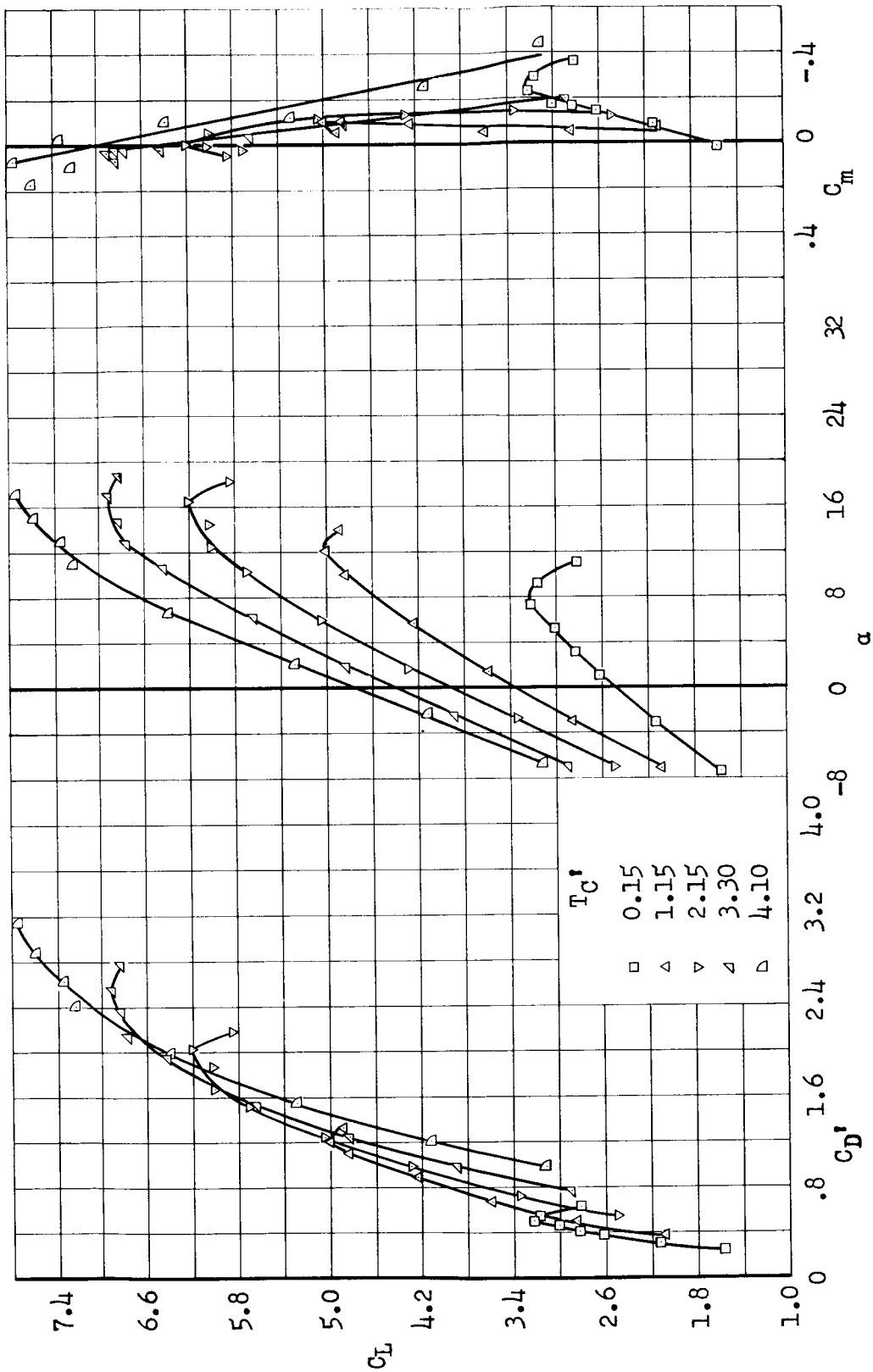

(j) $\delta_f = 40^\circ$; $\delta_a = 30^\circ$; $C_{\mu_f} = 0.024$; $C_{\mu_a} = 0.006$; $i_t = 4.3^\circ$.

Figure 5.- Continued.

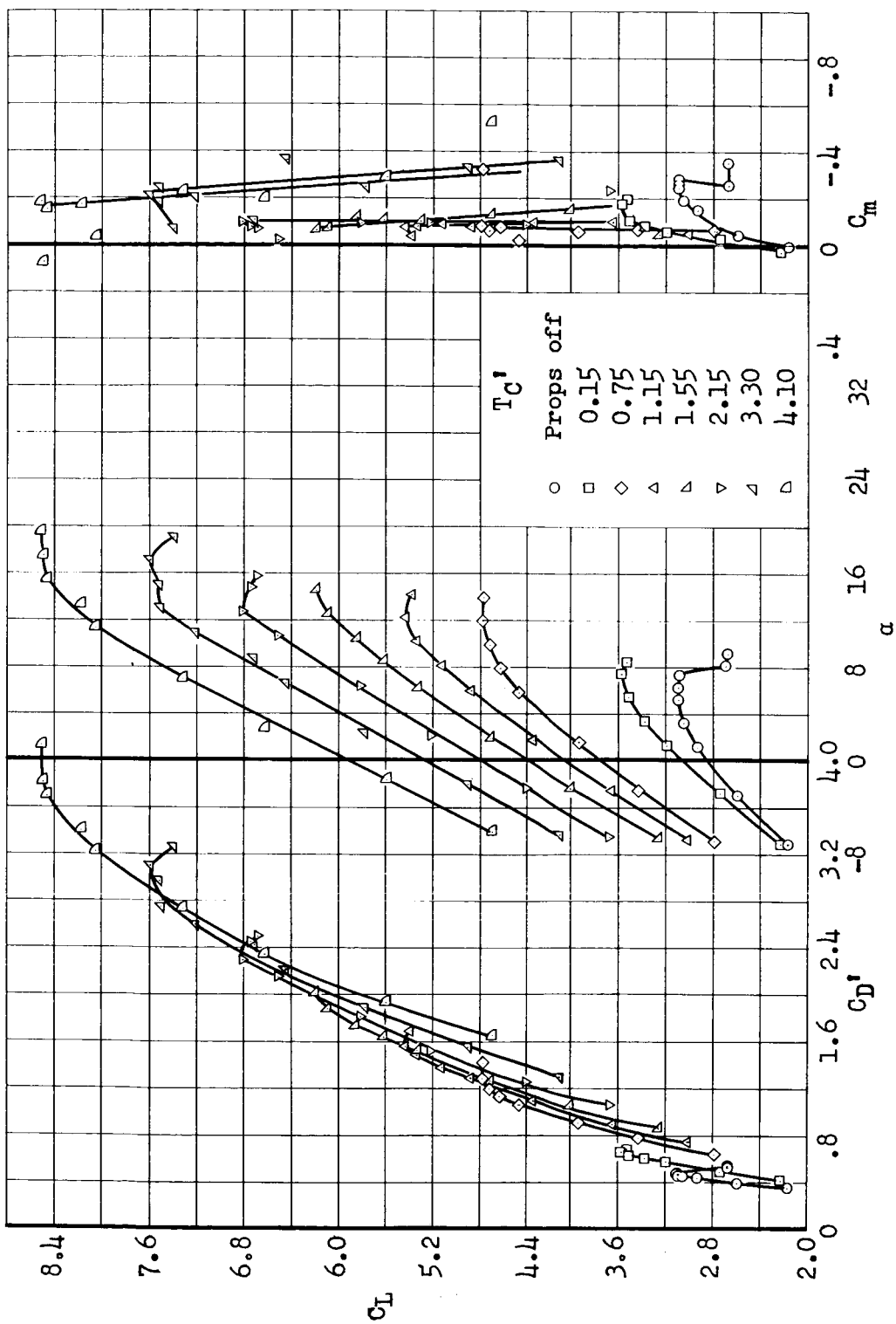

(k) $\delta_f = 60°$; $\delta_a = 30°$; $C_{\mu_f} = 0.029$; $C_{\mu_a} = 0.006$; $i_t = 4.3°$.

Figure 5.- Continued.

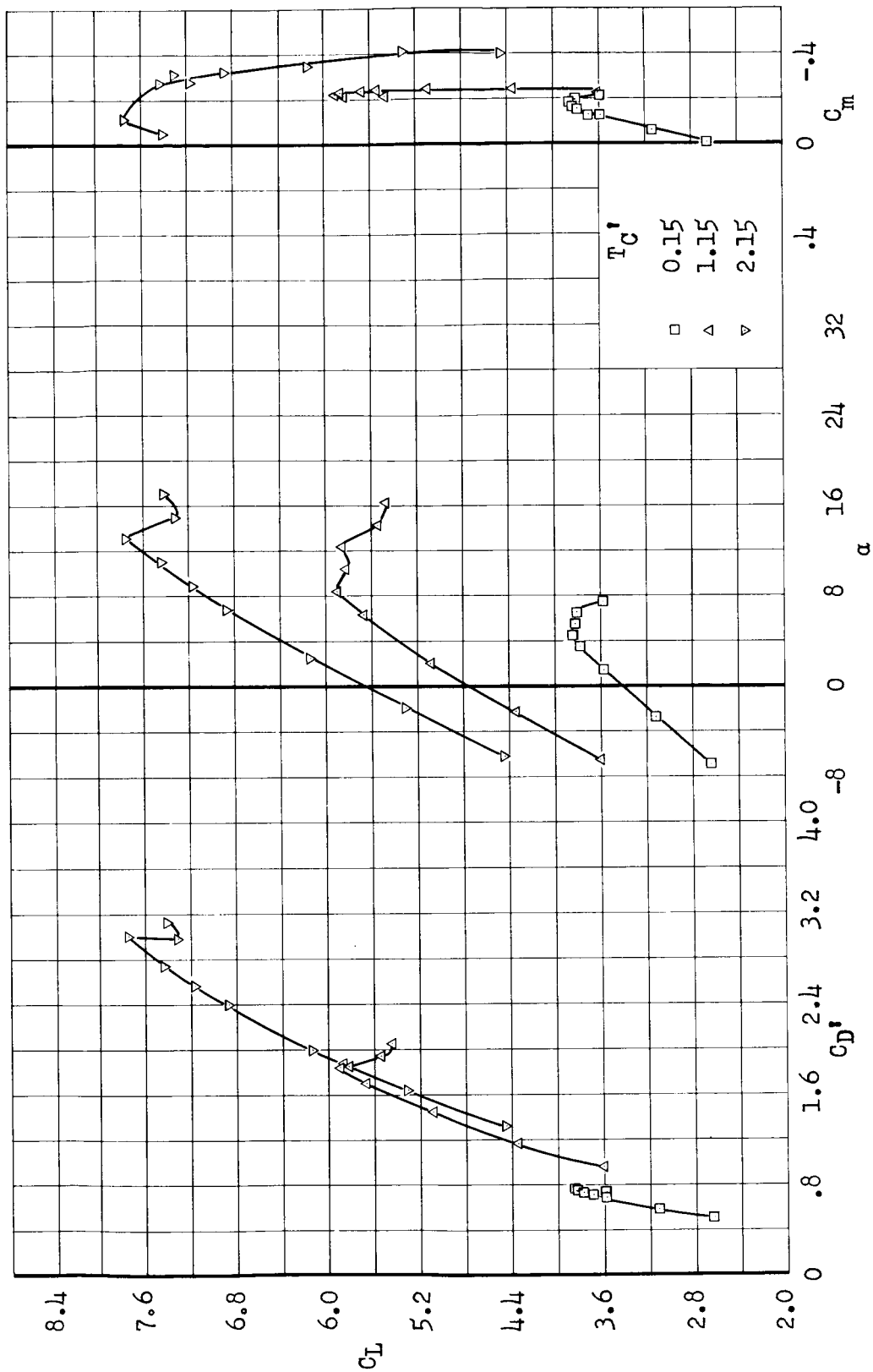

(l) $\delta_f = 60°$; $\delta_a = 30°$; $C_{\mu_f} = 0.080$; $C_{\mu_a} = 0.006$; $i_t = 4.3°$.

Figure 5.- Continued.

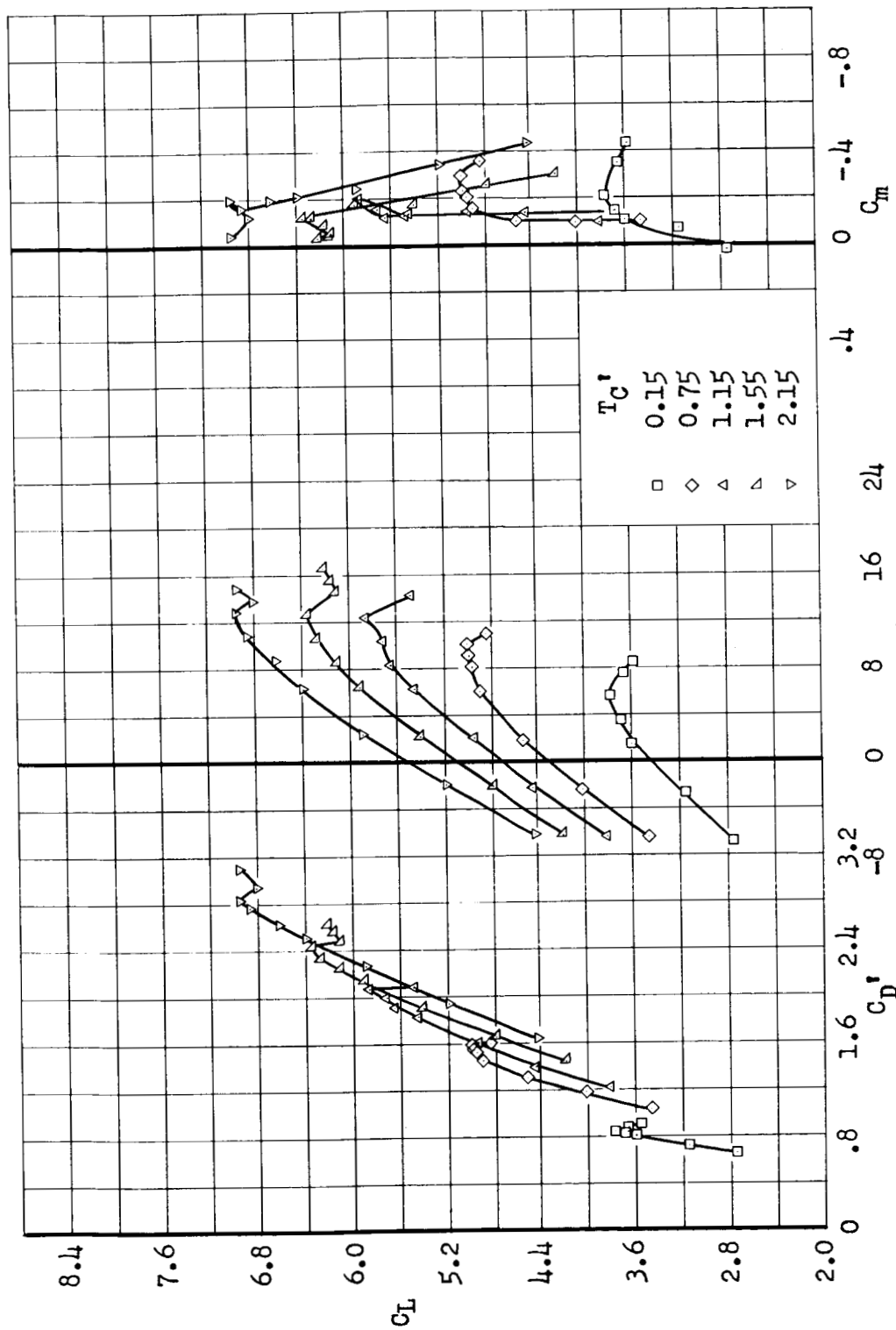

(m) $\delta_f = 80°$; $\delta_a = 30°$; $C_{\mu f} = 0.049$; $C_{\mu a} = 0.006$; $i_t = 4.3°$.

Figure 5.- Continued.

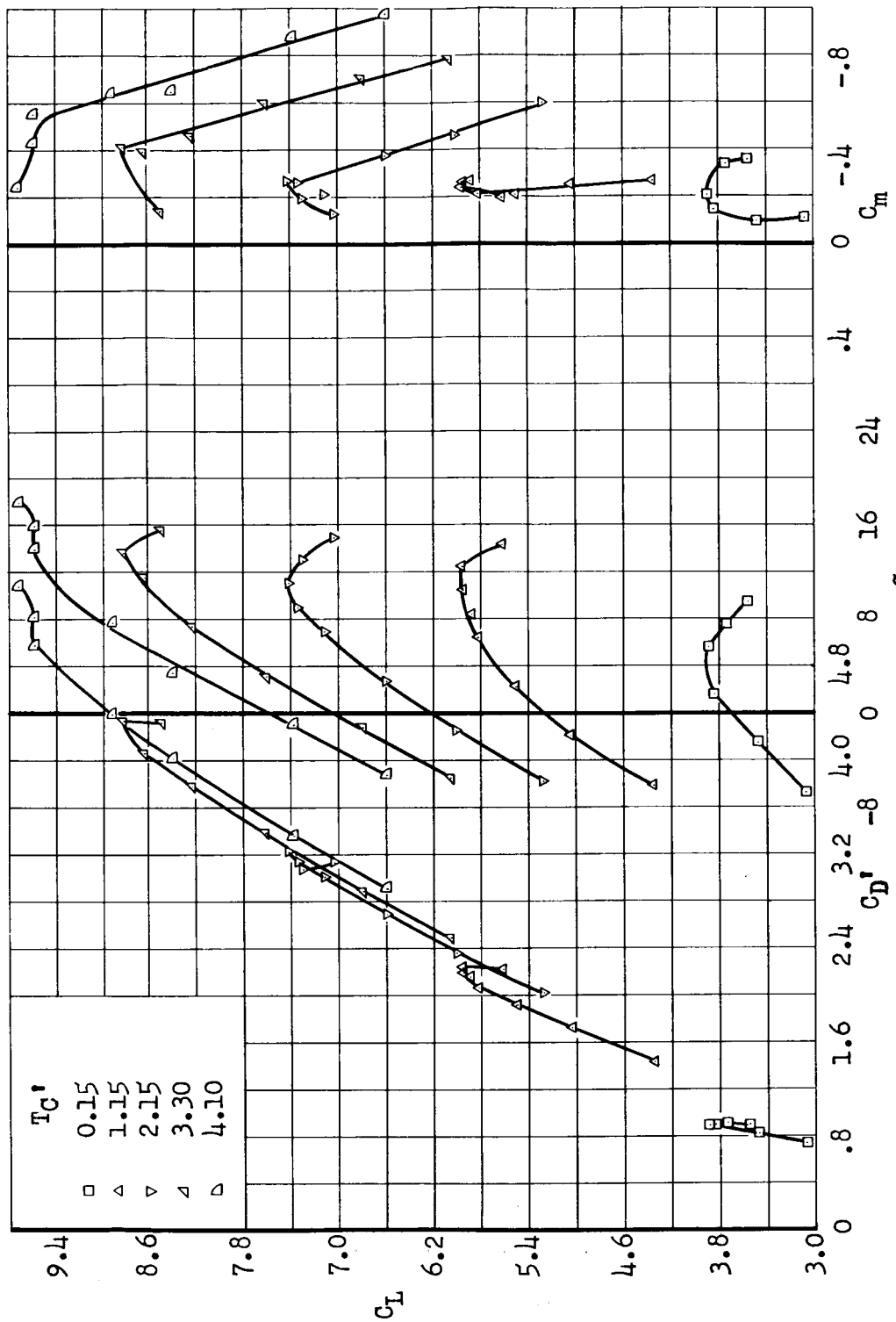

(n) $\delta_f = 80^\circ$; $\delta_a = 30^\circ$; $C_{\mu_f} = 0.08$; $C_{\mu_a} = 0.006$; $i_t = 4.3^\circ$.

Figure 5.- Concluded.

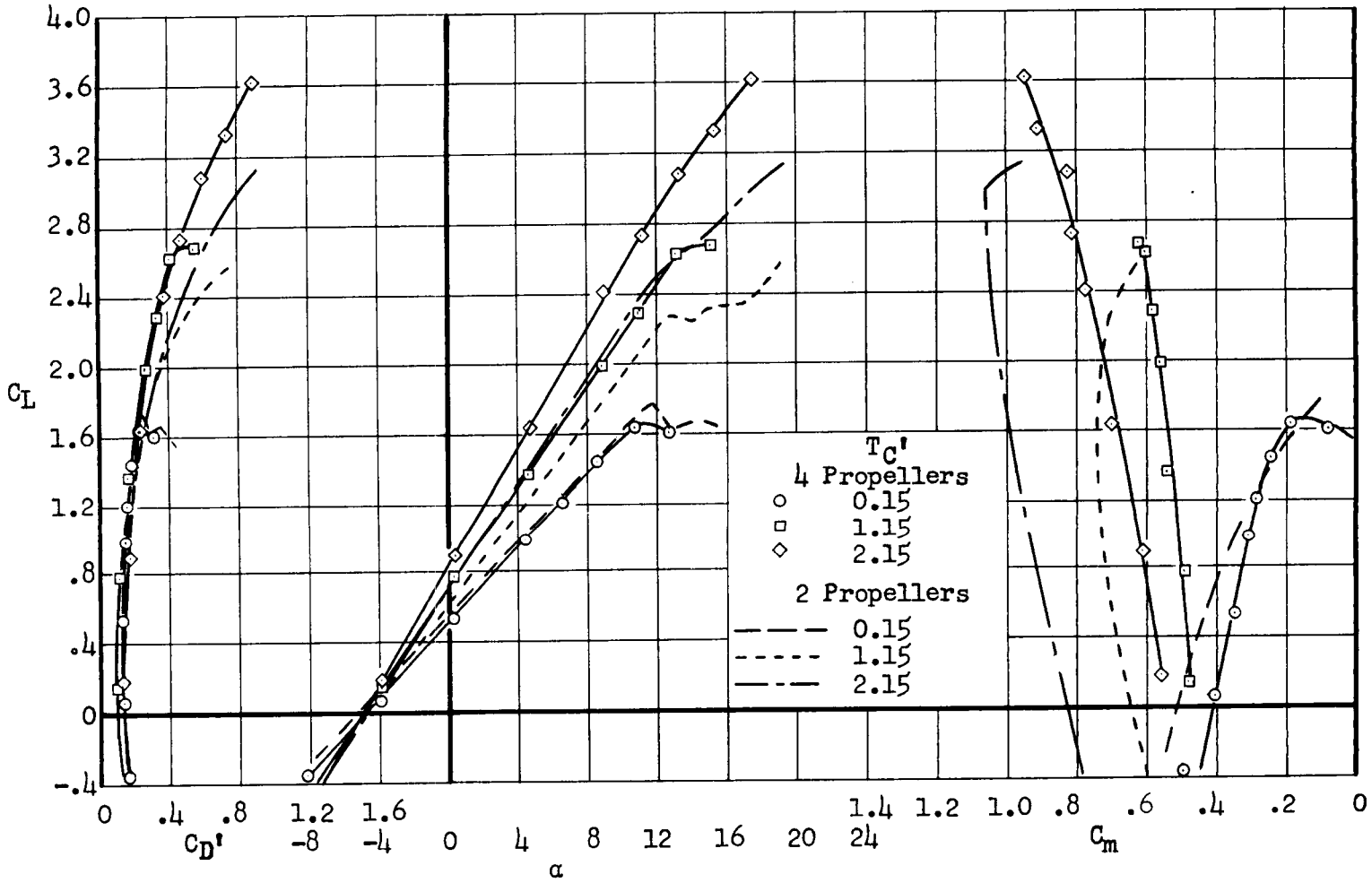

(a) $\delta_f = \delta_a = 0^\circ$; $C_{\mu_f} = C_{\mu_a} = 0$

Figure 6.- Effect of number of propellers on the aerodynamic characteristics of the model; $i_t = -3^\circ$.

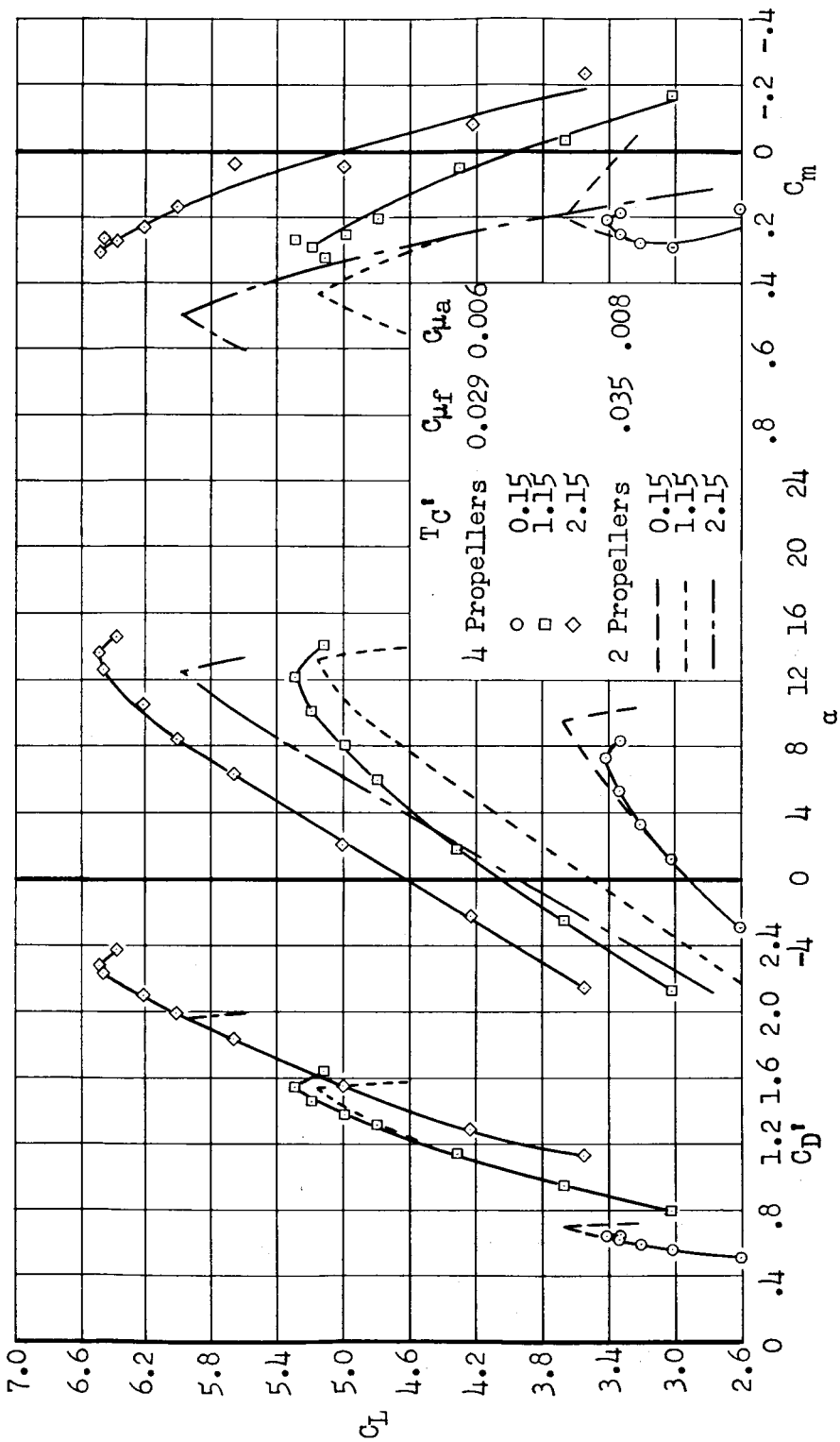

(b) $\delta_f = 60^\circ$; $\delta_a = 30^\circ$

Figure 6.- Concluded.

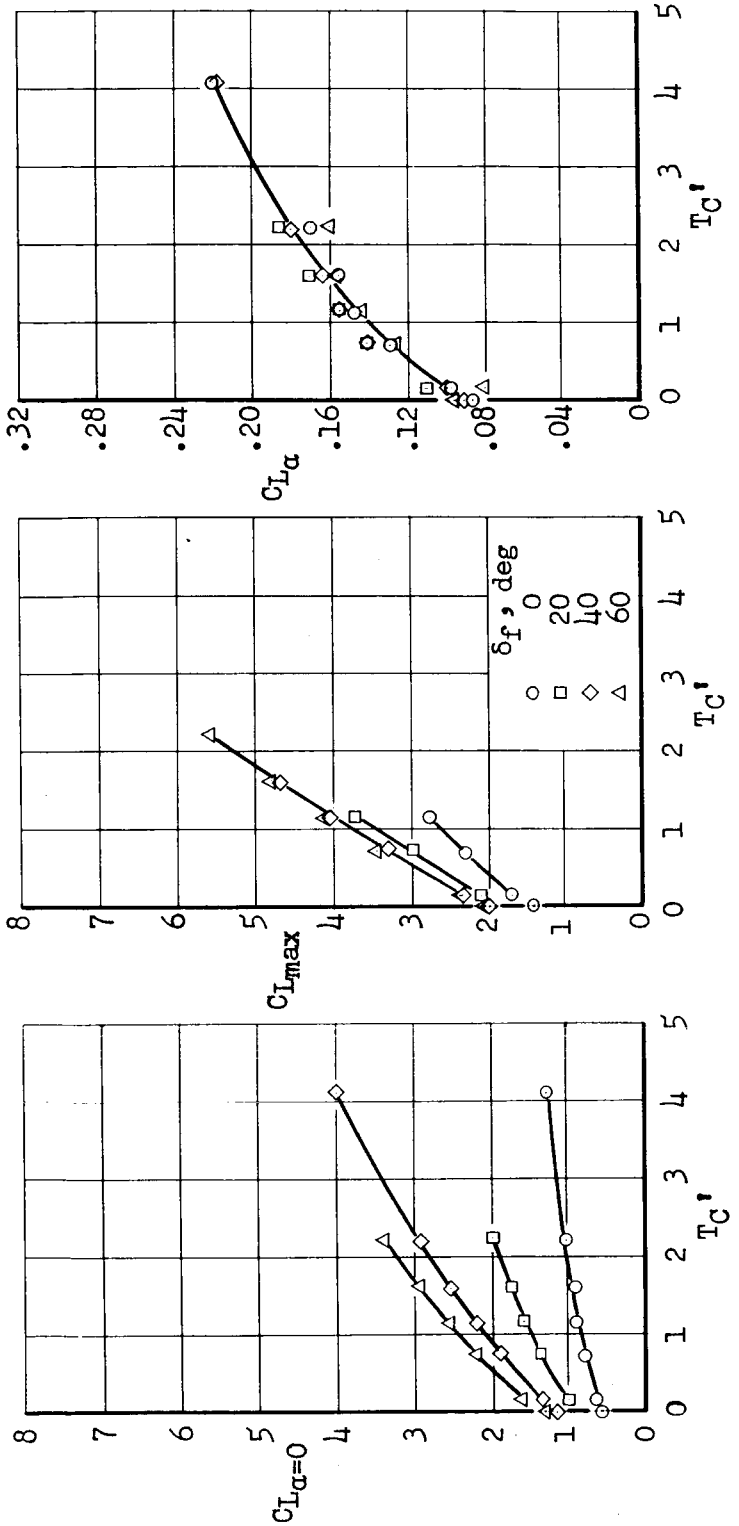

(a) $\delta_a = 0^o$; $C_{\mu_a} = C_{\mu_f} = 0$

Figure 7.- Effect of thrust on the lift characteristics of the model with tail off.

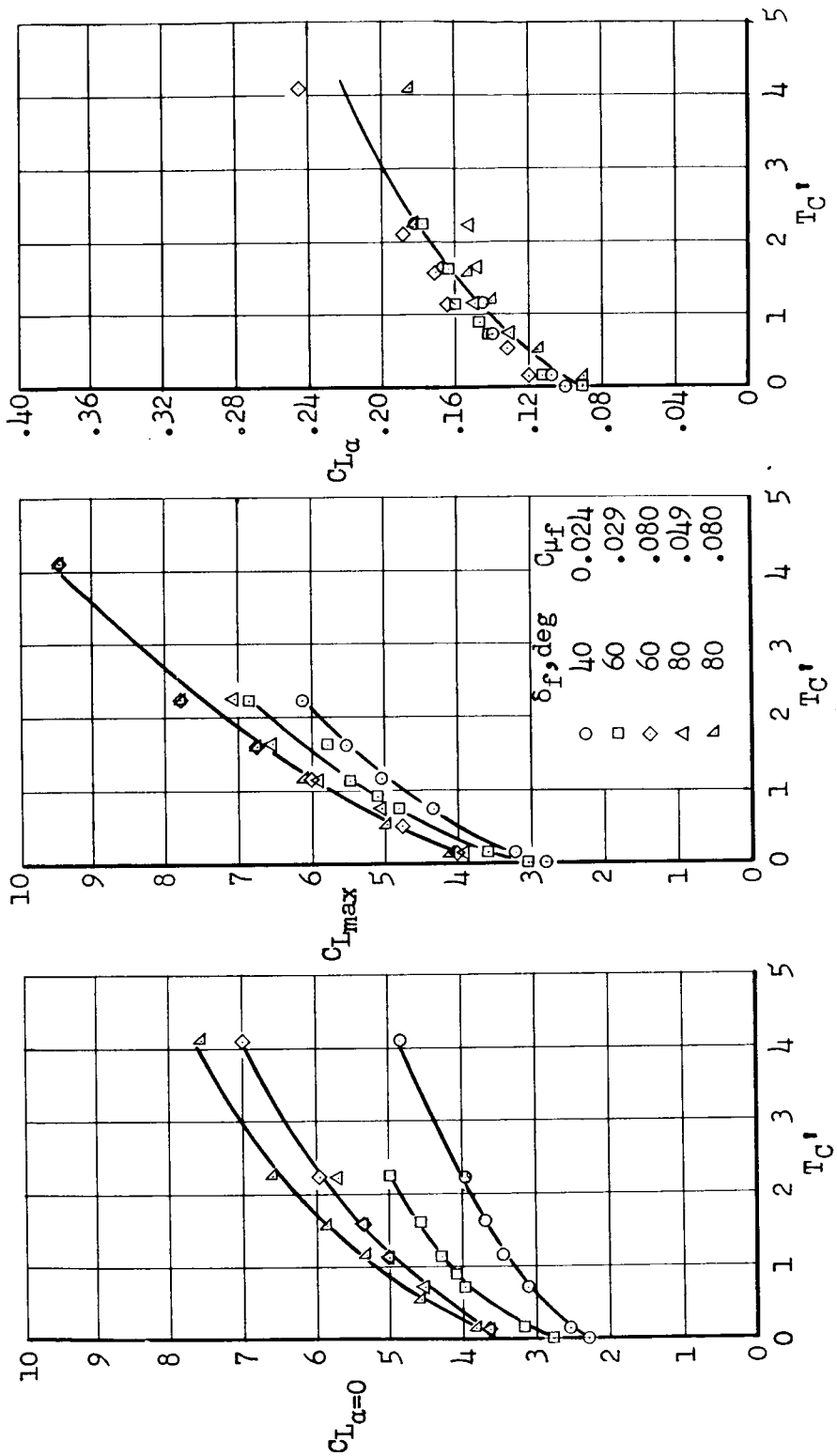

(b) $\delta_a = 30^o$; $C_{\mu_a} = 0.006$

Figure 7.- Concluded.

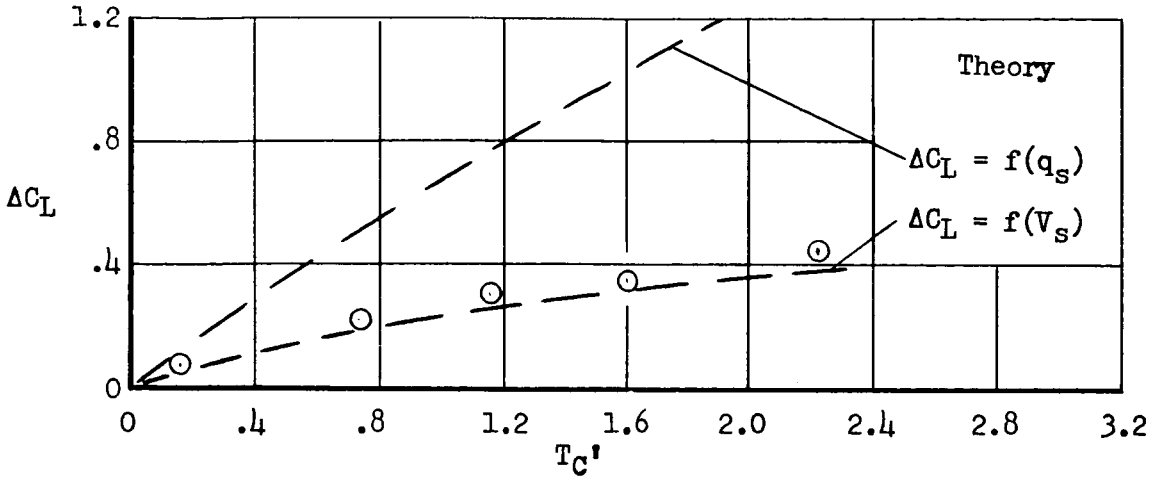

(a) $\delta_f = 0^\circ$; $\delta_a = 0^\circ$; $C_\mu = 0$; $C_{l_o} = 0.60$

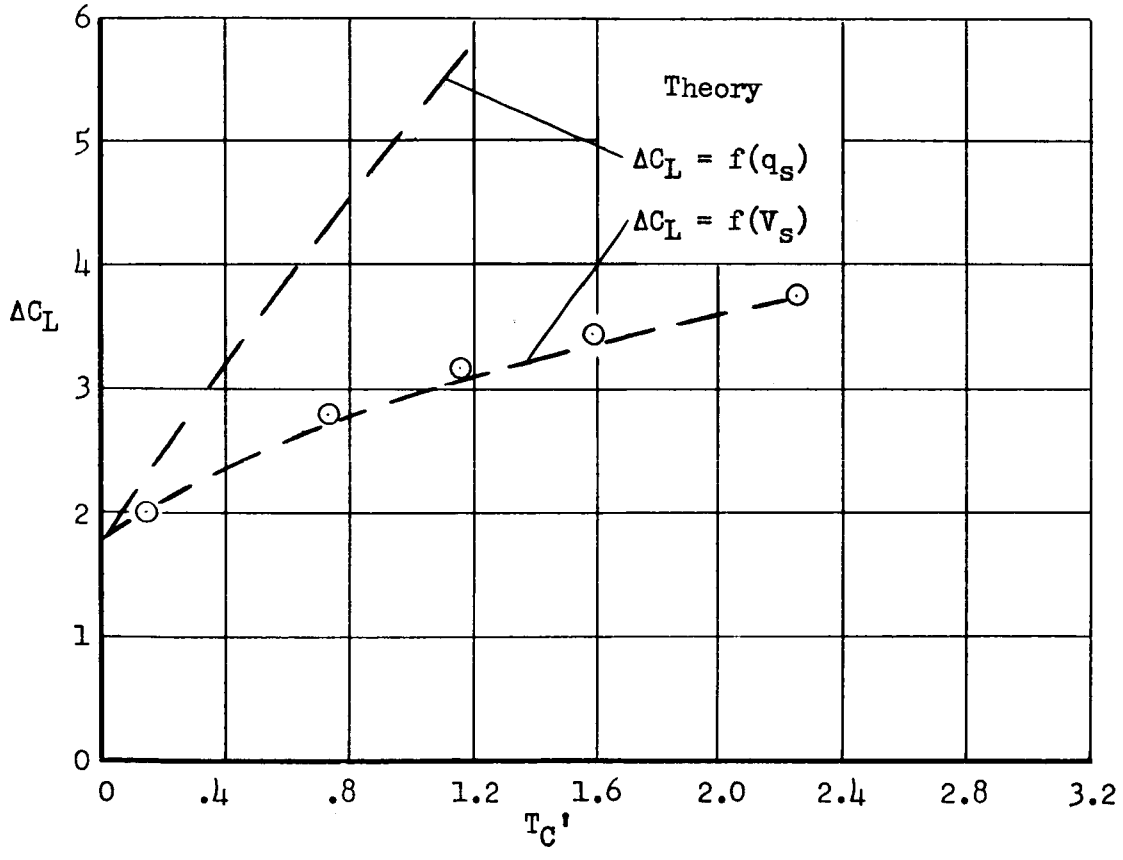

(b) $\delta_f = 60^\circ$; $\delta_a = 0^\circ$; $C_{\mu_f} = 0.029$; $C_{l_o} = 3.07$

Figure 8.- Comparison of the lift increment due to thrust with the theory of reference 1; $\delta_a = 0^\circ$, $\alpha = 0^\circ$.

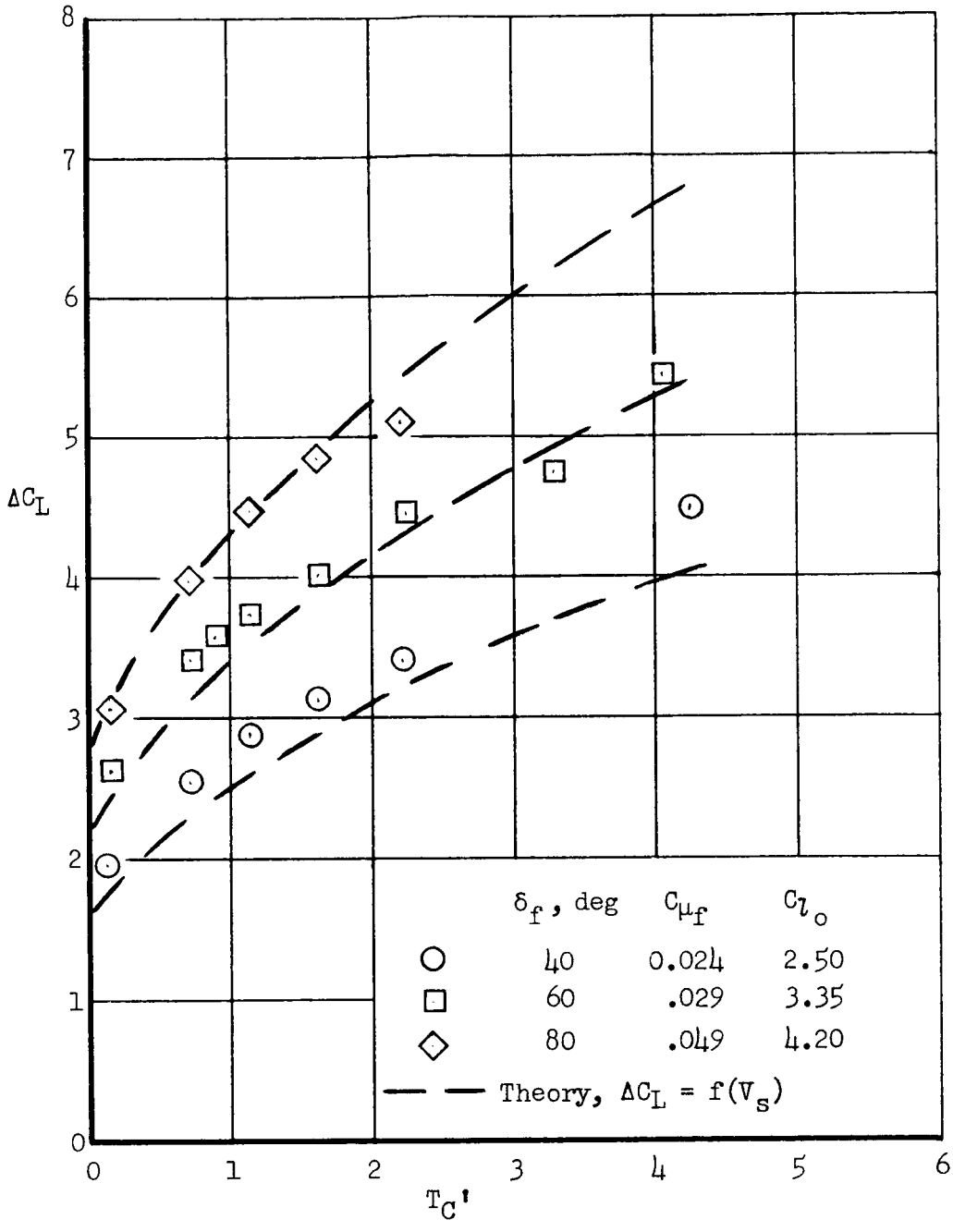

(c) $\delta_a = 30^o$; $C_{\mu_a} = 0.008$

Figure 8.- Concluded.

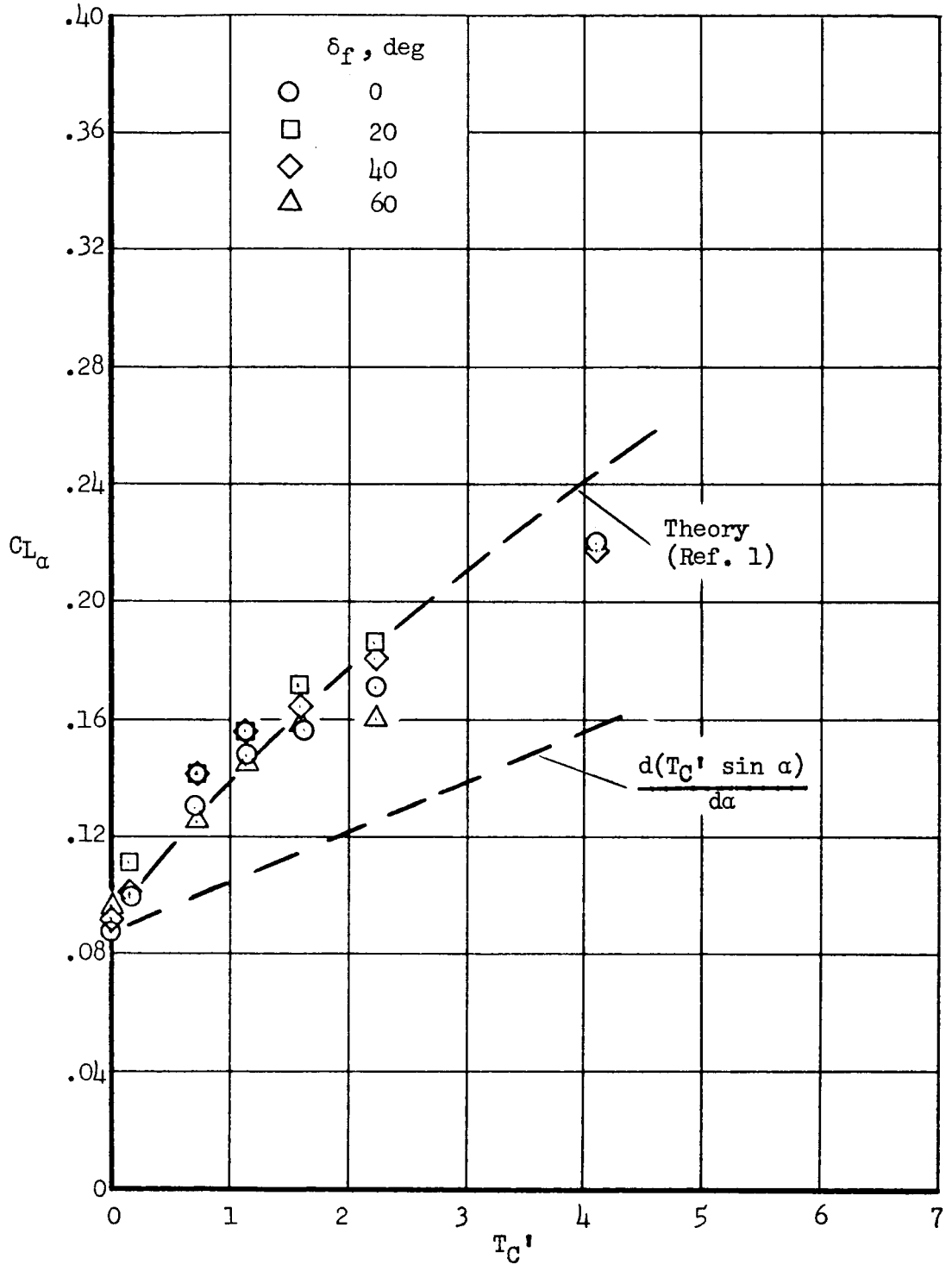

Figure 9.- Comparison of lift-curve slope with theory.

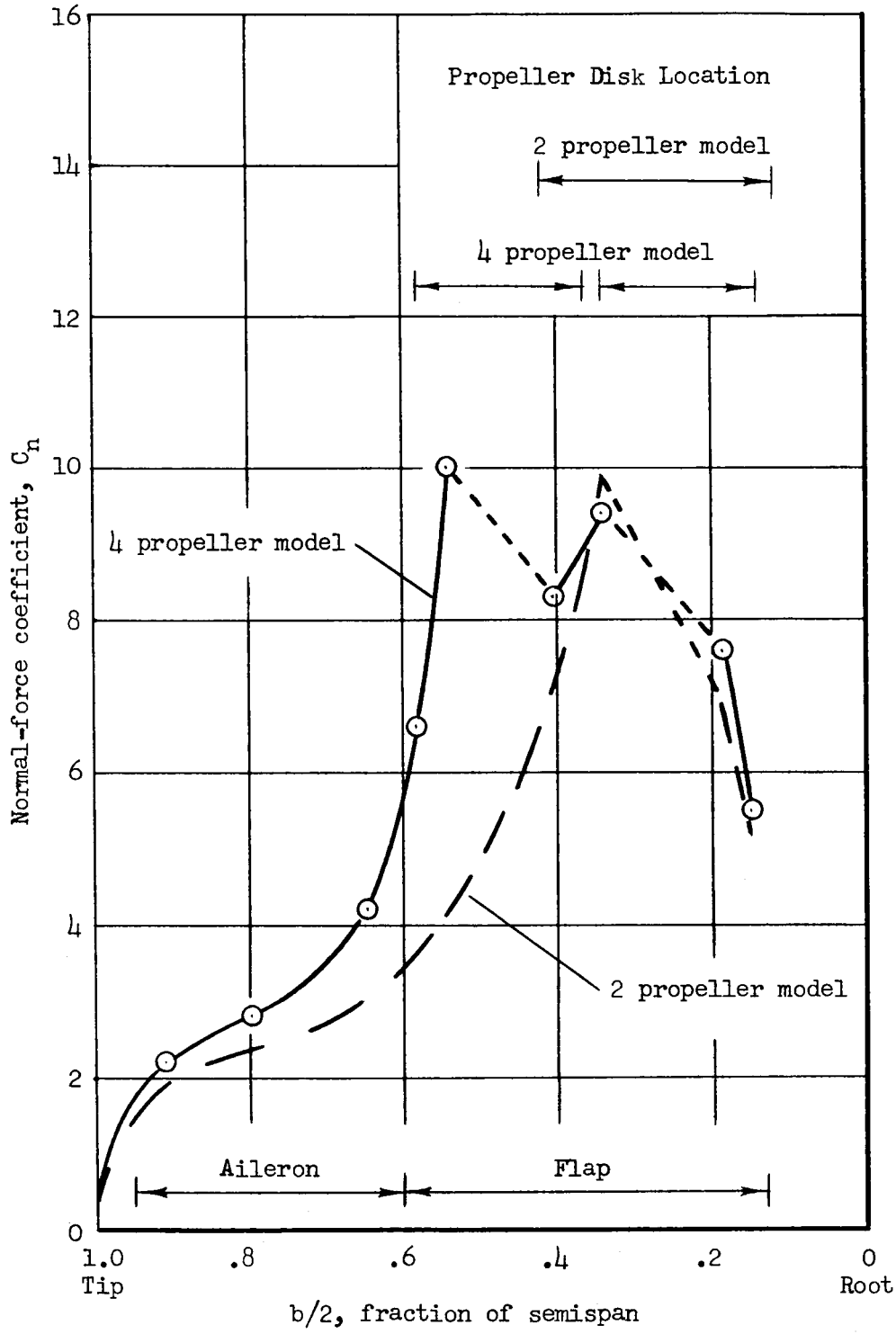

Figure 10.- Comparison of the loading on the left wing panel on the four- and two-propeller models; $\delta_f = 60^\circ$, $\delta_a = 30^\circ$; $C_{\mu_f} = 0.03$, $C_{\mu_a} = 0.006$, $\alpha_u = 0^\circ$, $T_C' = 2.2$.

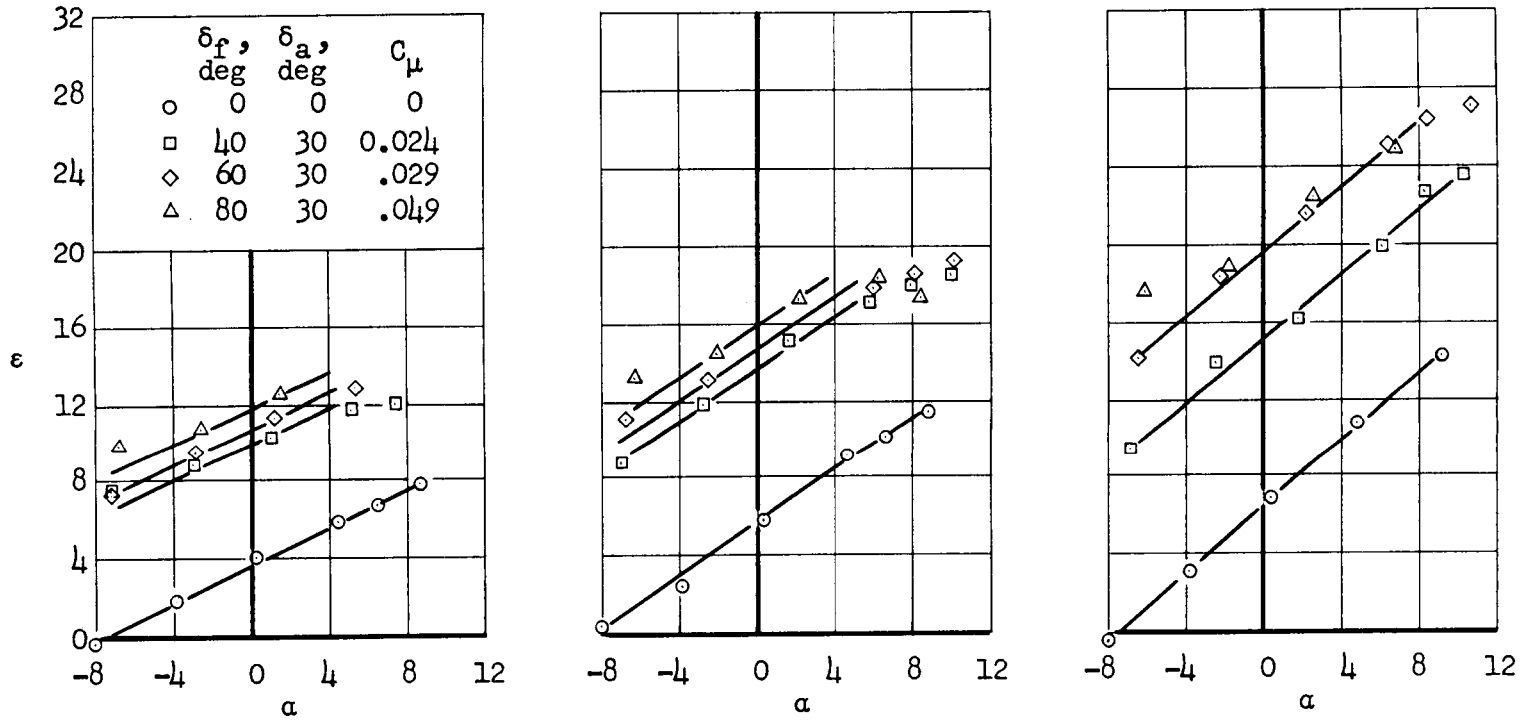

(a) T_C' = 0.15 (b) T_C' = 1.15 (c) T_C' = 2.15

Figure 11.- Variation of downwash with angle of attack.

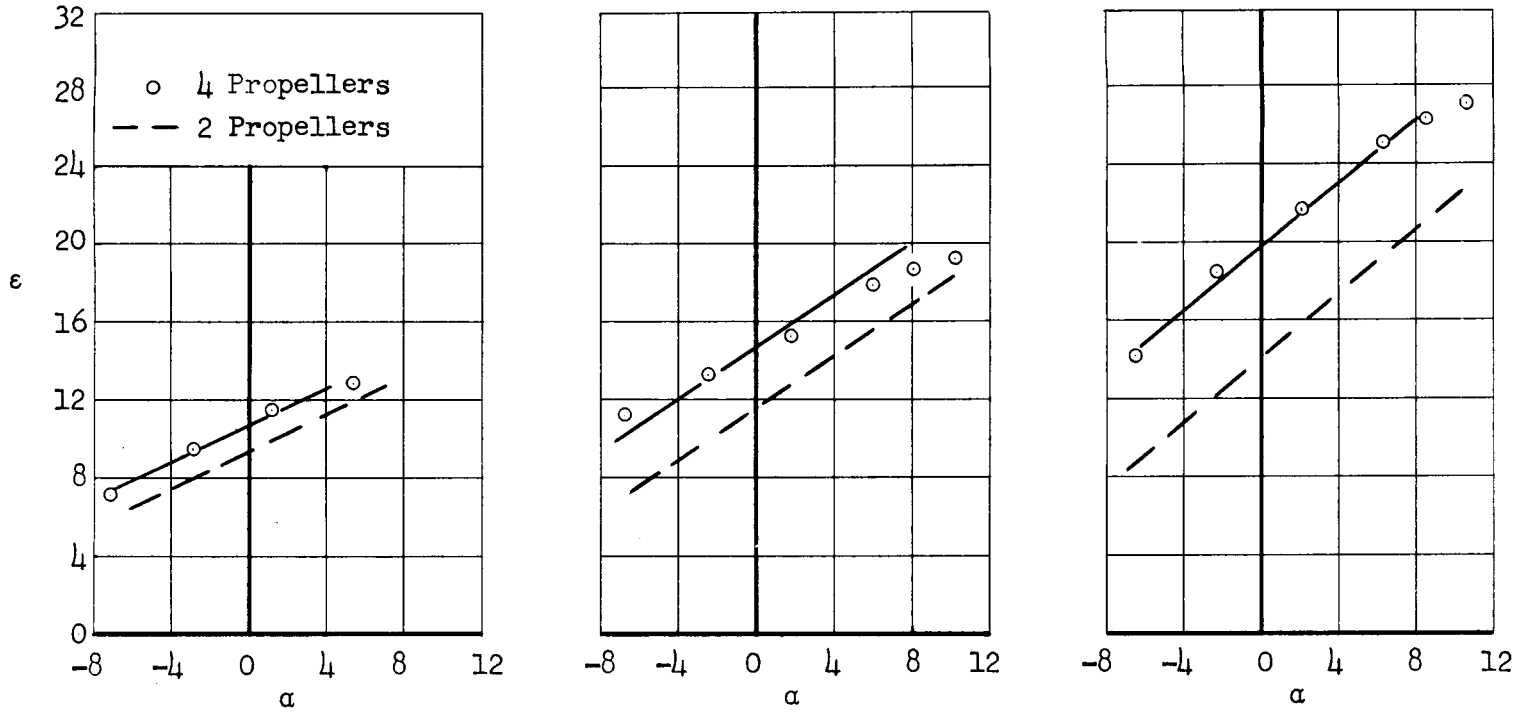

(a) $T_C' = 0.15$ (b) $T_C' = 1.15$ (c) $T_C' = 2.15$

Figure 12.- Comparison of the downwash at the tail for the two- and four-propeller models; $\delta_f = 60^\circ$, $\delta_a = 30^\circ$, $C_{\mu_f} = 0.03$, $C_{\mu_a} = 0.006$.

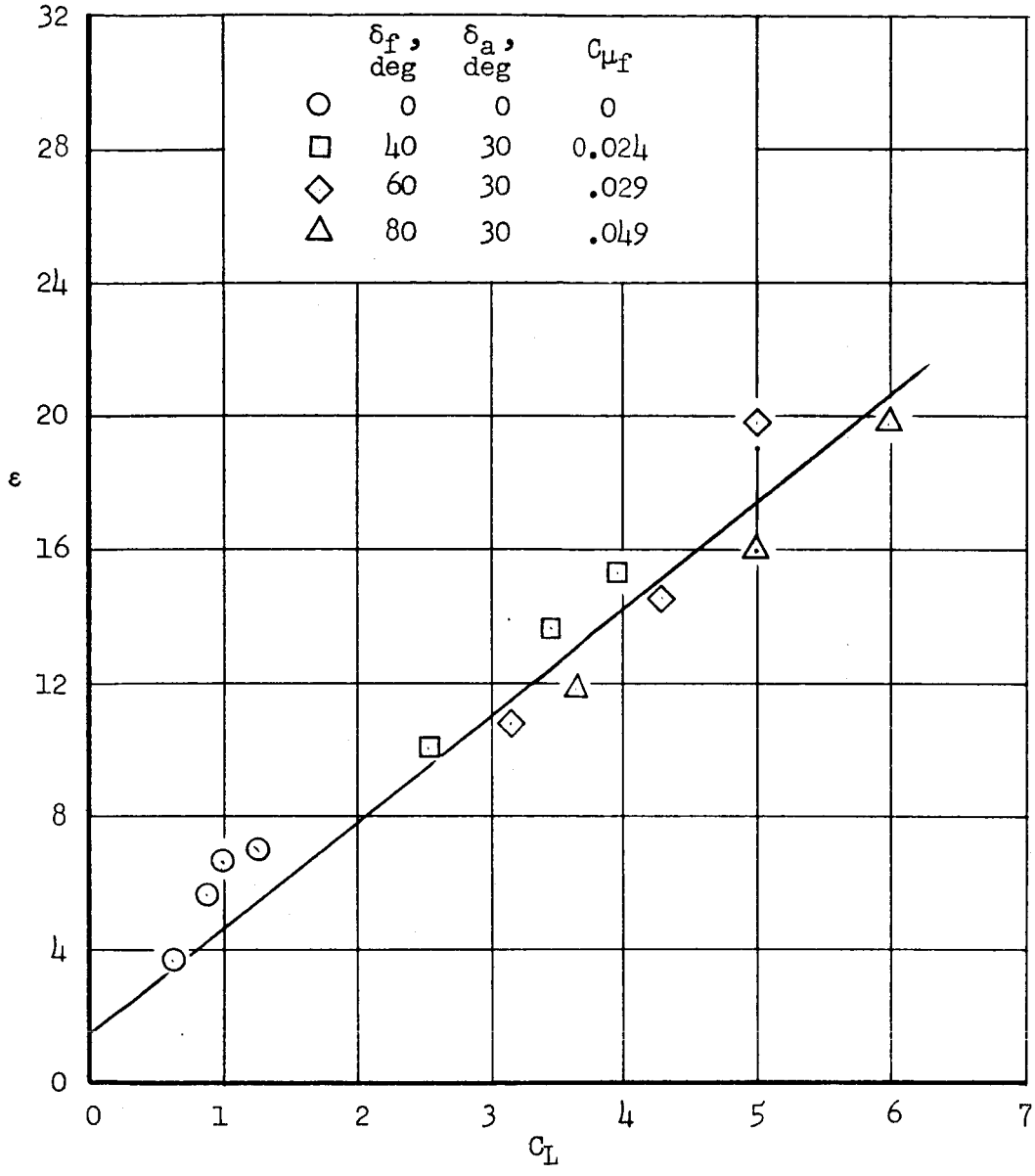

Figure 13.- Variation of downwash with lift coefficient.

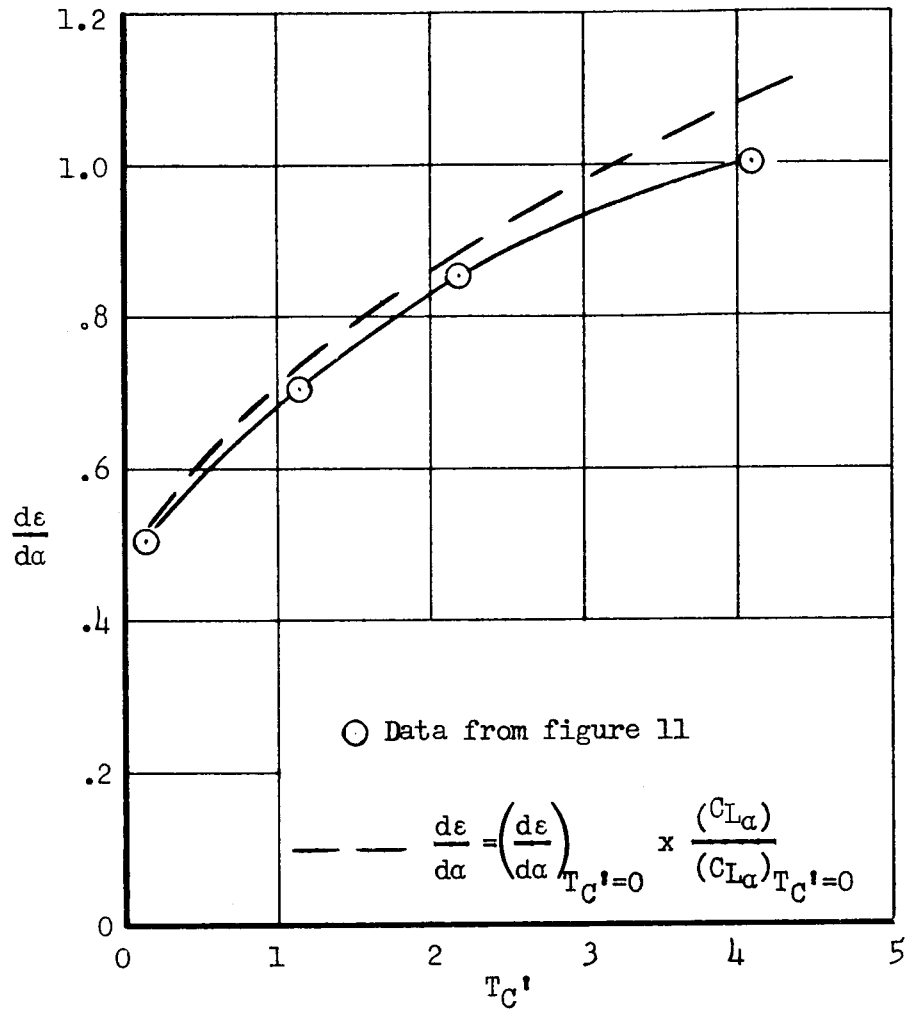

Figure 14.- Variation of downwash with thrust coefficient.

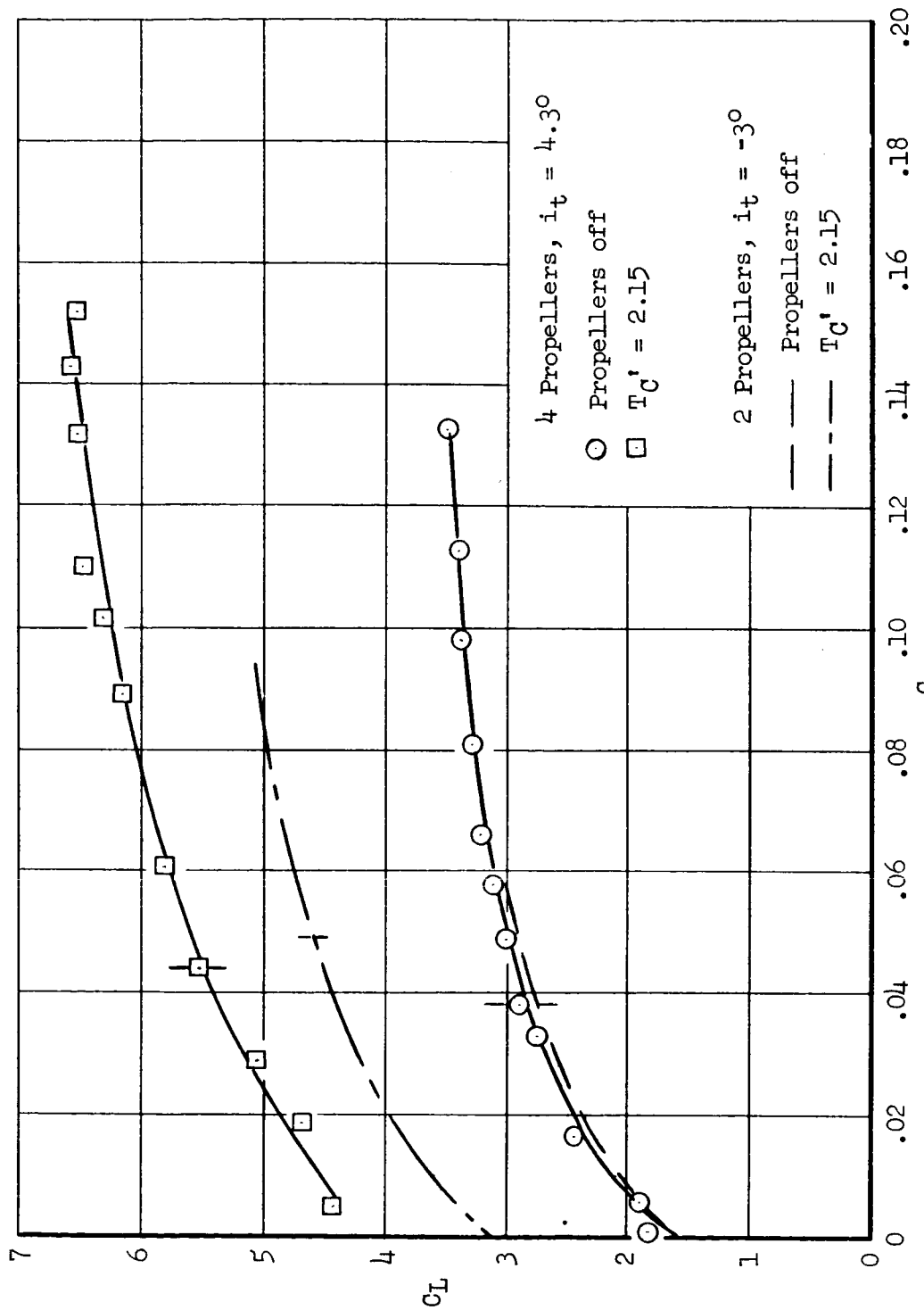

Figure 15.- Effect of number of propellers on the momentum flow requirements of the flap; $\delta_f = 60^\circ$, $\delta_a = 30^\circ$, $C_{\mu_a} = 0.006$, $\alpha_u = 0^\circ$.